Atmospheric Pollution Research 14 (2023) 101643

Contents lists available at ScienceDirect

Atmospheric Pollution Research

journal homepage: www.elsevier.com/locate/apr

# Lichen biomonitoring of airborne trace elements in the industrial-urbanized area of eastern algiers (Algeria)☆

Henia Saib [a,b], Amine Yekkour [c,d], Mohamed Toumi [b,e], Bouzid Guedioura [f], Mohamed Amine Benamar [g], Abdelhamid Zeghdaoui [b], Annabelle Austruy [h], David Bergé-Lefranc [a], Marcel Culcasi [a], Sylvia Pietri [a,h,*]

[a] Aix Marseille Univ, CNRS, ICR, UMR 7273, SMBSO, Marseille, France
[b] Laboratory of Ethnobotany and Natural Substances - Department of Natural Sciences, Ecole Normale Supérieure El-Ibrahimi Kouba, Algiers, Algeria
[c] Laboratory of Microbial Systems Biology, Ecole Normale Supérieure El-Ibrahimi Kouba, Algiers, Algeria
[d] National Institute of Agronomic Research of Algeria - Mehdi Boualem Station, Baraki, Algiers, Algeria
[e] Department of Natural and Life Sciences, Faculty of Sciences, University of Algiers, Algeria
[f] Reactor Division/CRND, Algeria
[g] Laboratory of Applied Physics, University Saad Dahleb, Blida, Algeria
[h] Institut Ecocitoyen pour La Connaissance des Pollutions, Fos-sur-Mer, France

ARTICLE INFO

*Keywords:*
Lichen biomonitoring
*Pseudevernia furfuracea*
Trace element pollution
Enrichment factor
Multivariate analysis

ABSTRACT

This study established a comprehensive picture of airborne metal pollution in the industrial urbanized area of the East of Algiers (Algeria). Thalli of the epiphytic lichen *Pseudevernia furfuracea* were transplanted from a remote unpolluted forest (Theniet El-Had) to eighteen biomonitoring sites in the Rouiba–Reghaia region exhibiting contrasting anthropogenic activities, including the wooded Reghaia Nature Reserve. Thirty-three metals and rare earths, and Br in lichen thalli were determined after 3 months exposure by X-ray fluorescence and instrumental neutron activation analysis. All biomonitored element concentrations exhibited dramatic increases compared to the control region, and calculation of contamination factor index unveiled that Sb, Pb, Ti, V, Ce, La, Ga, Cr, Cs, Cu, and Cd had the highest contamination levels in almost all the study sites. The degree of ambient pollution was assessed using enrichment factor, pollution load index, cluster analysis, and principal components analysis. A multiple correspondence analysis showed Pb, Sb, and Ga to be highly enriched with heavy contamination in all study sites, even in the Reghaia Nature Reserve.

## 1. Introduction

In the last decades airborne metal pollution has become a global environmental issue to be faced by public authorities due to increasing evidence of multiple adverse effects of trace elements on living organisms. For most metallic contaminants, the contribution of anthropogenic inputs has far outpaced that of natural sources and there is evidence that airborne particulate matter-bound species, including metals, accumulate in the human body to trigger chronic pathologies such as neurological degenerative processes, multiple sclerosis or muscular dystrophy (Rehman et al., 2018), and lung cancer (Swanton et al., 2022). Biosensors that have been extensively used to assess air pollution locally include lichens (Boonpeng et al., 2017; Demková et al., 2017; Dron et al., 2021), mosses (Zechmeister et al., 2005; Vuković et al., 2016), plant leaves or tree rings (Austruy et al., 2019).

Lichens are perennial organisms devoid of any root system or other

*Abbreviations:* RNR, Reghaia nature reserve; RU, Reghaia urban area; IZ, Industrial zone of Rouiba–Reghaia; TH, Theniet El-Had Region; CF, contamination factor; PLI, pollution load index; EF, enrichment factor; CA, Cluster analysis; PCA, principal component analysis; MCA, multiple correspondence analysis.

☆ This paper is dedicated to the memory of Prof. Mohammed Rahali, our dear colleague and friend.Peer review under responsibility of Turkish National Committee for Air Pollution Research and Control.

* Corresponding author. Aix Marseille Univ, CNRS, Institut de Chimie Radicalaire, UMR 7273, SMBSO; Centre Scientifique de Saint Jérôme, Service 522, Avenue Escadrille Normandie Niemen; F-13397 Marseille Cedex 20, France.

*E-mail addresses:* henia.saib@g.ens-kouba.dz (H. Saib), amineyek@gmail.com (A. Yekkour), toumi_m2001@yahoo.fr (M. Toumi), algeryfx@gmail.com (B. Guedioura), benamardz64dz@gmail.com (M.A. Benamar), zeghdaouiens@hotmail.fr (A. Zeghdaoui), annabelle.austruy@institut-ecocitoyen.fr (A. Austruy), david.BERGE-LEFRANC@univ-amu.fr (D. Bergé-Lefranc), marcel.culcasi@cnrs.fr (M. Culcasi), sylvia.pietri@univ-amu.fr (S. Pietri).

https://doi.org/10.1016/j.apr.2022.101643
Received 4 October 2022; Received in revised form 28 December 2022; Accepted 29 December 2022
Available online 30 December 2022

absorptive organs, protective cuticles, and filtration mechanisms, which maintain a uniform morphology over time with a high surface/volume ratio. These properties confer to lichens an exceptional ability to easily accumulate airborne pollutants, particularly metals, at levels exceeding their physiological needs to some extent (Conti and Cecchetti, 2001; Sorbo et al., 2008; Osyczka et al., 2018). Consequently, lichens are commonly used in air quality studies and heavy metal biomonitoring through measurement of pollutants levels accumulating in their thalli in the long term, in the area where these species grow (Bari et al., 2001; Aslan et al., 2013; Paoli et al., 2015; Ratier et al., 2018; Massimi et al., 2019).

However, such studies are hardly realizable using endogenous lichens under conditions of unusual dramatic pollution bursts or extended periods at high levels that outperform their homeostatic efficiencies and

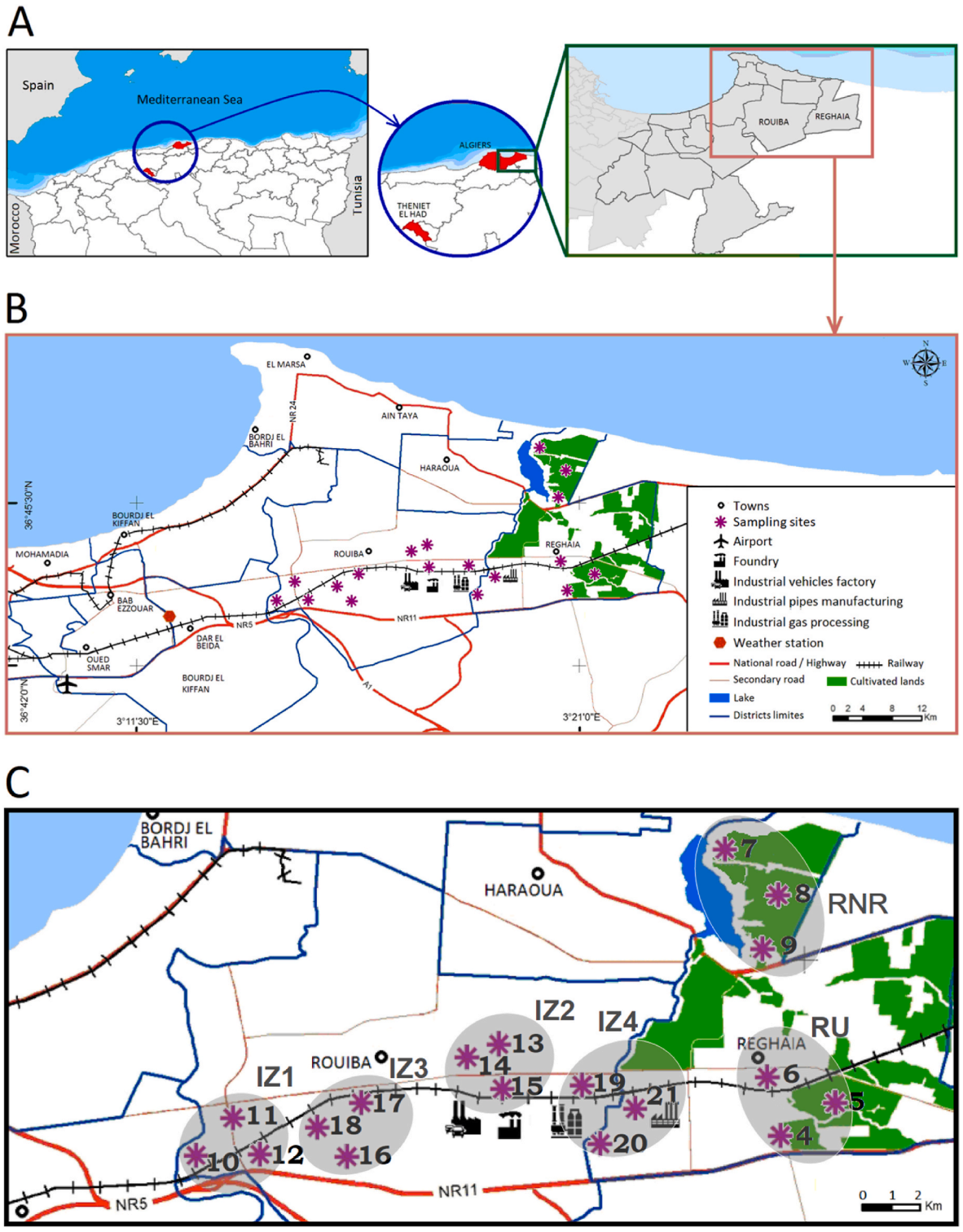


**Fig. 1.** (A) General map of the Rouiba–Reghaia region (Eastern of Algiers) showing the unpolluted Theniet El-Had area (TH). (B) Enlargment showing the location of the main eighteen sampling sites (*) in the industrial-urbanized region. (C) Typologies of the six studied areas (RU, RNR, and IZ1–4; gray backgrounds) as obtained by cluster analysis of trace elements contents (see Fig. 2A). Arabic numbers refer to the sampling site coordinates presented in Table S1.

reduce their abundance (Agnan et al., 2017). To keep the advantage of using lichen pollution biosensors in conditions and/or areas where these species are scarce or absent, alternative transplant techniques have been proposed (Basile et al., 2008; Nannoni et al., 2015; Paoli et al., 2015). Globally, this involves relocating thalli from an area deemed as uncontaminated to remote sites under study for a short period of time, and it has been shown such lichens transplants to be good quantitative probes of atmospheric heavy metals distribution (Boamponsem et al., 2010, 2017; Incerti et al., 2017; Kodnik et al., 2017; Zhao et al., 2019) and powerful witnesses of the effectiveness of anti-pollution regulations (Lucadamo et al., 2022).

In Algeria, lichen-based biosensing of trace element contamination, as well as an accurate knowledge of atmospheric metallic pollutants concentrations in the main industrial and urban areas are still scarce. Previous lichen studies have documented only a limited number of airborne metal elements such as Pb in Algiers and Annaba (Rahali, 2002; Semadi, 1994), Pb and Zn in Tiaret (Maatoug et al., 2010) or a group of 10 heavy metals in the Bordj Bou Arreridj area (Adjiri et al., 2018).

The aim of this study was to present the first detailed inventory of atmospheric heavy metal contamination in the Rouiba–Reghaia region, one of the largest, very active, and populated urban-industrial areas of Algeria (East of Algiers, Fig. 1A) where autochthonous lichens are yet poorly available. The macro lichen *Pseudevernia furfuracea* (L.) Zopft v. *Furfuracea* was used as a transplanted biomonitor for a large set of 33 rare earths and metal elements accumulating during a three months exposure period in eighteen sites, including a wooded nature reserve. Lichens, which were presumably subjected to low, medium or high levels of atmospheric pollution, were compared to samples transplanted in the unpolluted Theniet El-Had National Park Forest control region. Further, two approaches were performed to discriminate between anthropogenic (industry, traffic) and natural (crustal materials, marine aerosols) sources of trace metals, i.e., by determining the enrichment factor for each individual element, and by performing multivariate statistical techniques.

Altogether, the data acquired here enabled: (i) the build-up of a database of atmospheric pollution in three contrasting environments, i.e., rural, urban, and industrial sites, and (ii) to validate the usefulness of *Pseudevernia furfuracea* lichen as an enhanced pollution biomonitoring species for an array of airborne metals.

## 2. Materials and methods

### 2.1. Study area, monitoring sites, and meteorological conditions

The studied region of Rouiba–Reghaia, located at 30 km from the East of Algiers, represents a suburban area where agricultural, industrial activities, and road traffic are preponderant and have constantly increased over the past 30 years. In this surface area of about 2600 ha, eigtheen random sampling stations were established in order to account for the contribution of each of the main local metal emission sources, including the intense railway and road traffics, and were located along a presumed increasing pollution gradient (Fig. 1B). Eighteen monitoring stations were designed as follows: (1) the Reghaia Nature Reserve (RNR; 3 sampling sites) according to the Ramsar Convention 2003 located in a wooded area including a lake, (2) the Reghaia Urban area (RU; 3 sampling sites), a densely populated zone (estimated at 2700 inhabitants per $km^2$) with an important demographic growth, and subjected to the influence of local emissions, agriculture, railway and road traffic of the city, and (3) the industrial Rouiba–Reghaia zone (IZ1−4; 12 sampling sites, see Fig. 1B−C), one of the largest industrial areas in the country (1000 ha) with 250 mechanical, metallurgical, chemical and food processing units implanted along the railway. Lichens were then submitted to various sources of pollution, notably the high density of road traffic, the influence of agricultural and multiple industrial pollution sources from Reghaia, as well as the proximity of the Dar El Beïda airport (Fig. 1B). Geographical coordinates of each site are reported in the Supplementary materials (Table S1). The locations of industrial facilities are often intertwined with residential neighborhoods. On the basis of census data in Wilaya–Algiers, the city had a population of 155,710 inhabitants in 2015. Moreover, this urban-industrial region also includes the East−West highway (A1), three main national roads (NR5, NR11, and NR24), and the Algiers−Blida railway (Fig. 1B).

Globally, the region is characterized by a Mediterranean climate, with a mild winter with heavy rainfall and a hot and dry summer with an arid period extending from the midst of May until the end of September. According to the data from the local meteorological station of Dar El Beida (2008–2018), the annual average of precipitation is 660 mm, the temperature ranges 12.0–24.3 °C with an average of 18.1 °C and a relative humidity of 74%. The prevailing frequent winds are from the North and North−East, with an average wind speed of 10.4 m/s. The station of Algiers is located at the inferior sub-humid bioclimatic stage of the temperate winter.

Three additional monitoring stations distant of at least 10 km each other were established in the Theniet El-Had National Park Forest (TH). This area (700 m above sea level), located 200 km from the Rouiba−Reghaia area in northwestern Algeria (Fig. 1A), was taken as a relatively unpolluted control site in the study. With a surface area of 3500 ha and a mountain peak standing at 1787 m (Ras El-Braret), the TH consists of vast forests of Atlas cedars (*Cedrus atlantica*) with diverse flora and fauna of value.

### 2.2. Lichen sampling and transplantation procedures

The fruticose epiphytic macro lichen *Pseudevernia furfuracea (L.)* Zoft v. *Furfuracea* was chosen since it is largely employed in biomonitoring studies with transplants (Sorbo et al., 2008; Malaspina et al., 2014). Thalli of seemingly healthy lichens from the clean TH area were carefully collected with adhering bark substrate from mature *Cedrus atlantica* trees having similar sizes, at 1.5–2.5 m above the ground and all around each tree to minimize contamination by soil and any influence of prevailing winds. Samples, excluding over and densely isidiate thalli, were transferred to the laboratory in individual polyethylene bags, and then carefully cleaned from foreign materials and debris. The thalli were manipulated as promptly as possible to avoid any source of stress. Before transplantation, samples vitality was checked by analyzing their photosynthetic efficiency by measuring chlorophyll fluorescence (Garty et al., 2000).

One day after sample collection, about 150 thalli were transplanted to the 21 monitoring sites according to the procedure of Cuny et al. (2001). Thalli were arranged on 20 × 40 cm wooden boards (3 thalli per board, technical replicates) and three of these boards were installed at each studied site on three trees separated by at leat 5 m each other (triplicates), as illustrated in Fig. S1 (Supplementary materials). Once transplanted, the lichens were kept in the monitoring sites for an optimal duration of 3 months for pollution measurements (Frati et al., 2005; Gallo et al., 2014; Lucadamo et al., 2016), in winter period (January–April), an ideal season for lichen growth in Algeria, before being collected for trace element analysis.

### 2.3. Sample preparation and trace element analysis

Following collection experimental lichens were carefully cleaned using plastic tweezers to remove dusts and residue, and then placed in small Pyrex Petri dishes without prior washing (Saiki et al., 1997; Boonpeng et al., 2017). Afterwards, they were oven-dried at 80 °C for at least 48 h, crushed and homogenized in a grinding mill, and sieved through a 2-mm pore size mesh. The recovered powder was stored at ambient temperature before analyses. A diversity of methods are available for elemental analysis of lichens, including atomic absorption spectroscopy, inductively coupled plasma-mass spectroscopy, INAA, and XRF. Here, INAA (see 2.3.1) and XRF (see 2.3.2) were selected because they are both powerful non-destructive multielemental techniques

(Herrero Fernández et al., 2015; Pantelica et al., 2016).

#### 2.3.1. Instrumental neutron activation analysis (INAA)

INAA, one of the most sensitive and accurate techniques for trace elements determination, was applied for quantifying one halogen (Br), and a series of heavy metals and rare earths including Al, In, Mn, Ti, V, As, Ba, Co, Cu, Cr, Cs, Hf, Fe, Ga, La, Ce, Nd, Sm, Eu, Tb, Yb, Lu, Hg, Rb, Sb, Sc, Se, Th, U, and Zn. Irradiation procedures were carried out using the NUR research reactor at the Draria Nuclear Research Center in Algiers (Algeria). Three sub-samples, each containing 100 mg of lichen powder, standards, and blanks, were weighed, heat-sealed in polyethylene bags and packed in high-purity (99.99%) aluminum foil for irradiation. For the determination of short-lived radionuclides (i.e., Al, In, Mn, Ti, V), lichen samples, standards, and blanks were simultaneously irradiated for 200 s in the pneumatic transfer system under a thermal neutron fluence rate of $5.4 \times 10^{12}$ $cm^{-2}$. $s^{-1}$. For the analysis of longer-lived radioisotopes (i.e., As, Ba, Br, Co, Cu, Cr, Cs, Hf, Fe, Ga, La, Ce, Nd, Sm, Eu, Tb, Yb, Lu, Hg, Rb, Sb, Sc, Se, Th, U, and Zn), the irradiation scheme involved irradiation for 18 h under a neutron fluence rate of $2.7 \times 10^{13}$ $cm^{-2}$ $s^{-1}$ (Guedioura et al., 2014; Bouhila et al., 2015). For short irradiated samples, gamma-ray counting was carried out after a decay time of 300 s while for long irradiated samples two successive countings were performed after a decay period of 1 day and 7–10 days, respectively. Gamma-ray counting was carried out using a hyper-pure germanium (HPGe) detector (Mirion Technologies (Canberra), Montigny-le-Bretonneux, France). HPGe detector main characteristics, spectral processing, calculations and quality controls using Tulip sample (IPE-175) and epiphytic lichen material (IAEA-336) as certified standards are given in the Supplementary materials.

Concentrations were expressed on a dry weight (dw) basis. Samples were analyzed in duplicate and the instrumental limits of detection were found as follows (in $\mu g.g^{-1}$ dw): Al, 84.6; As, 0.19; Ba, 0.61; Br, 0.28; Co, 0.04; Cu, 0.1; Cr, 0.08; Cs, 0.17; In, 0.05; Fe, 7.33; Ga, 0.61; Hf, 0.09; La, 0.1; Ce, 0.14; Nd, 0.90; Sm, 0.01; Eu, 0.01; Tb, 0.01; Yb, 0.04; Lu, 0.005; Mn, 12.9; Hg, 0.04; Rb, 0.1; Sb, 0.06; Sc, 0.002; Se, 0.1; Ti, 0.5; V, 0.62; Th, 0.10; U, 0.01, and Zn, 1.31.

#### 2.3.2. X-ray fluorescence spectroscopy (XRF)

X-ray fluorescence spectroscopy analysis, an accurate technique for quantifying environmentally important heavy metals such as Cd and Pb in lichens, was performed at the Applied Physics Laboratory of Blida University (Algeria). An X-ray fluorescence spectrometer (Malvern Panalytical Epsilon 3XLE, Palaiseau, France), with silicon drift detectors (SDD with Peltier effect, resolution 132.6 keV for Kα-Mn X-ray) and X-ray tube excitation (primary target Ag, 50 kV; Malvern Panalytical) was used according to Rekik et al. (2016). X-ray spectra were identified using the Epsilon 3 XL software (version 1.3.A. (8.24), 2014). The yields of the characteristic X-ray peaks (Kα-Cd, Lα-Pb) were quantified after adjustment and subtraction of the background noise. Elements contents were determined by the Omnian process with various filters (Cu-500, Al-200, Al-50, Ti, Ag) and without filters and compared to IPE175 and IAEA-336 standards irradiated under the same conditions.

For INAA and XRF analysis the results of the quality controls on certified materials are given in Tables S2 and S3 (Supplementary materials).

### 2.4. Calculation of environmental indexes of pollution

To estimate the air pollution level within the study area, calculations of several environmental indexes of air pollution were performed for each element and monitoring site, such as contamination and enrichment factors, and pollution load index.

#### 2.4.1. Contamination factor

The contamination factor (CF) was calculated to estimate the atmospheric contamination level of each element in each monitoring site as follows:

$$CF = Cs/Cc \quad (1)$$

where Cs is the mean concentration of each element in the transplanted lichens at a given monitoring site and Cc is the corresponding average concentration at the TH control site (triplicates of the values obtained in 3 independent locations in TH).

Ranges of CFs were categorized into the following four contamination classes according to Boamponsem et al. (2010), as [CF range, contamination]: [< 1.2, none]; [1.2–2, light]; [2–3, medium], and [≥ 3, heavy]. For each element at the TH control site, a CF value of 1 is taken as the background level.

#### 2.4.2. Pollution load index

The pollution load index (PLI) was calculated as follows:

$$PLI = (CF_1 \times CF_2 \times CF_3 \times CF_4 \times \ldots \times CFn)^{1/n} \quad (2)$$

where CF is the contamination factor of each selected element and *n* refers to the number of studied elements.

According to Boonpeng et al. (2017) a PLI value < 0.9 indicates an unpolluted area, whereas PLI ranges >1 were assigned to the following pollution levels: 1.1 < PLI <1.5, low; 1.5 = PLI <2.0, moderate; 2.0 = PLI <2.5, high; PLI ≥2.5, very high.

For each element recovered at the TH control site a background PLI value of 1 was taken.

#### 2.4.3. Enrichment factor

The enrichment factor (EF), commonly used as an index to distinguish whether trace elements recovered in lichen samples may originate from either natural or anthropogenic sources (Pacheco and Freitas, 2009), was calculated as follows:

$$EF = \left(C_e/C_R\right)_{Sample} / \left(Ce/C_R\right)_{Crust} \quad (3)$$

where $C_e$ is the concentration of the studied element and $C_R$ is the concentration of the reference.

The $(C_e/C_R)_{Sample}$ ratio was calculated using concentrations in lichen samples and the $(C_e/C_R)_{Crust}$ ratio was calculated as the average elemental richness in the Earth's crust, using the CRC upper continental crust manual (Lide, 2005). Then, EF was calculated for each element, with Al taken as a reference, since it rarely enters the atmospheric aerosols from anthropogenic sources (Reiman and de Caritat, 2000; Kłos et al., 2011; Agnan et al., 2015; Wu et al., 2020). According to Xiong et al. (2017), an EF based classification of elements was established as follows: [class; EF range; grade]: [class 1; ≤1, rare], soil and crust sources; [class 2; 2–10, mild], natural and anthropogenic; [class 3; 10–100, moderate], only anthropogenic); [class 4; 100–1000, high], artificial, and [class 5; >1000, extreme], artificial.

### 2.5. Statistics and data analysis

Data were analyzed by several statistical methods using FactoMineR R package 3.5.2 (Lê et al., 2008). Differences between element concentrations at TH control vs. each monitoring site were analyzed by a one-way analysis of variance (ANOVA) and Dunnett's post-hoc test for mean comparison. Differences were considered significant when $P < 0.05$.

In order to focus on lichen trace elements concentration at each sampling site and to estimate the pollution level, a data matrix of mean concentrations was constructed. Standardized data were computed to account for scale differences as documented earlier (Bozkurt, 2017; Incerti et al., 2017). The matrix was submitted to cluster analysis (CA) using Euclidean distance and complete linkage algorithm as previously described (Brunialti and Frati, 2007; Demiray et al., 2012) and principal component analysis (PCA). For interpretation purpose PLI was included

in the PCA as supplementary variable (i.e., plotted in the multivariate space, but not used to calculate the principal components) as proposed (Legendre and Legendre, 1998).

To estimate the pollution impact of selected elements over sites a multiple correspondence analysis (MCA) was performed by considering the experimental CF and EF data in a complete disjunctive matrix as a binary 'dummy variable' assuming values 1 or 0 according to their corresponding categorical class indicator (Greenacre, 2017) given in 1.4.1 (for CF) and 1.4.3 (for EF).

## 3. Results

One of the main interests of this study was to determine the spatial distribution of an array of 33 relevant airbone contaminants accumulated in thalli of *P. furfuracea* transplants in the area of Rouiba–Reghaia, as a consequence of anthropic pollution sources such as industrial activities, urbanization, road traffic, and agriculture. On the basis of the set of the measured trace elements content, a preliminar cluster analysis (CA) which aimed at splitting the twenty-one sampling sites into a number of different reasonable homogeneous groups, such that similar sites are placed in the same groups, was undertaken to judge the global inter-sites differences. As shown in Fig. 2A, in addition to the TH control

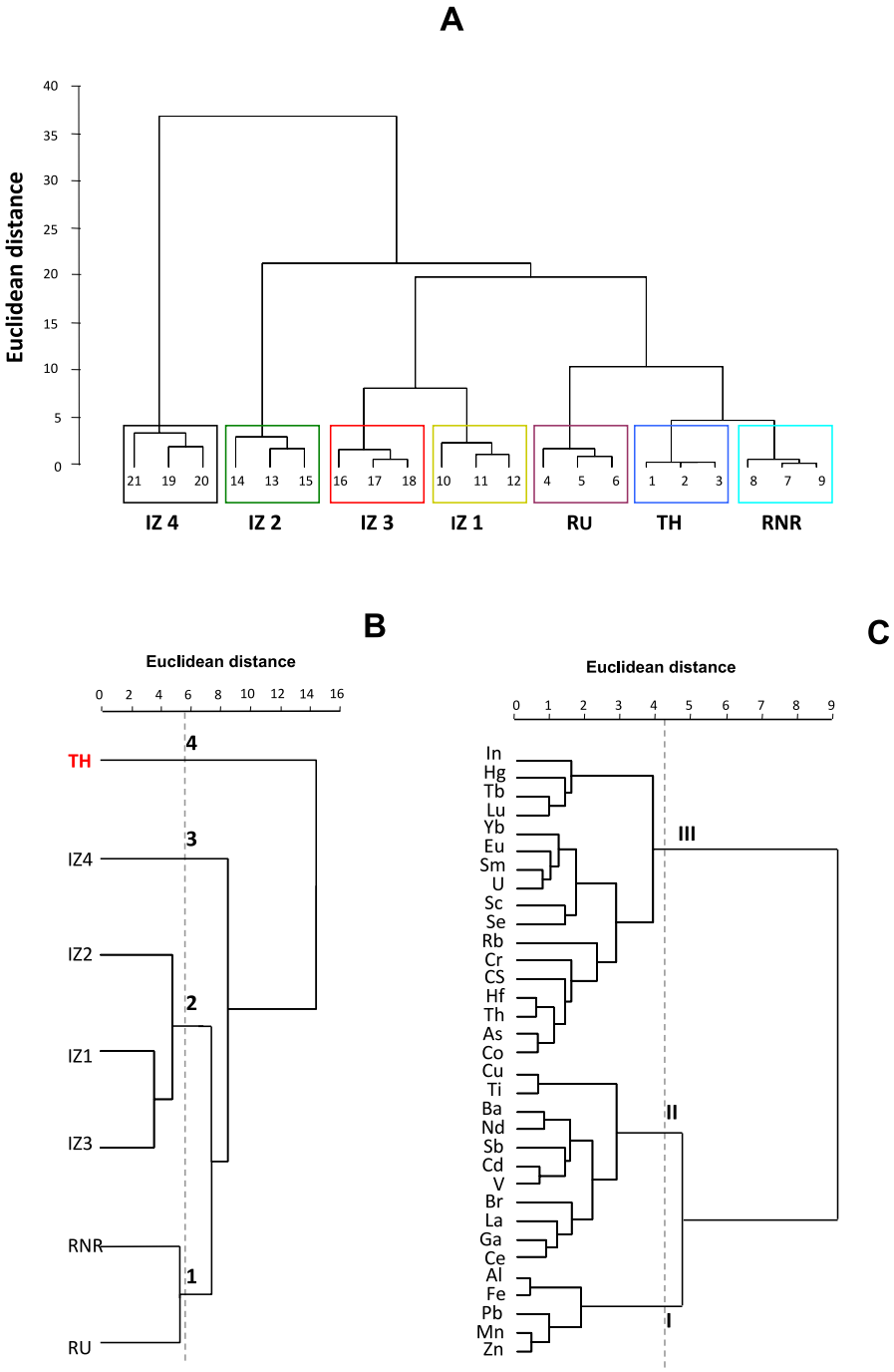


**Fig. 2.** Dendrograms obtained by cluster analysis of (A) the 21 sampling sites, (B) the seven studied areas, and (C) the 33 monitored elements. Arabic (1–4) and roman (I–III) numerals refer to Clusters of sites and groups of elements, respectively. Cluster analysis was performed from the measured metal concentrations in lichens in the six monitoring sites as compared to the unpolluted TH area (in red).

area, six homogeneous groups (RU, RNR, IZ1−4), were obtained by grouping the means from the 18 sampling sites having the same typology over the studied zone. Accordingly, for the further analysis of the study data, each group was considered as a homogeneous "studied area" defined by a mean content for each trace element.

### 3.1. Spatial variations in the accumulation of trace elements in lichen transplants

Table 1 shows the mean concentrations of 33 trace elements in transplanted lichens after a 3-month exposure in the six monitoring urban−industrial sites defined above, in comparison with background values from native in situ lichens transplanted in the unpolluted TH control site. Among the elements monitored in the industrial sites IZ1−4, seventeen of the metals and rare earth elements, including Cd, Cu, Cs, Ga, Sb, Pb, V, and Ti and, in a lesser extent, Cr, Al and Zn, were found at concentrations up to 890-fold higher than those found at TH ($P < 0.05$ or less). For most of the studied elements concentrations peaked in the IZ4 area, located in the vicinity of mixed anthropogenic pollution sources including a foundry, several factories, roads and railway traffic (Fig. 1C). While IZ4 region exhibited the most elevated concentrations of Al, Cd, Cu, Ga, Cs, La, Cr, Sb, Pb, V, Ce, Hf, Sm, Lu, Eu, Yb, Th, and U other elements including Mn, Ti, Zn, Br, and Co were found noticeably higher at IZ2 site. However, among the assayed metals the highest concentrations of Fe, Tb, and Sc were found at IZ1 site, while Nd and In levels culminated locally in lichens transplanted at IZ2,3 sites.

In transplants from the urban area RU, eighteen elements exhibited high concentrations, especially Ti, Cu, Rb, and Ga whose levels were found 190−350-fold higher that in control TH site. Strikingly, fifteen elements (especially Ti, Ga, Cu, and Cd) were found at high concentrations (30–120 fold higher than TH) in the RNR (Table 1).

### 3.2. Contamination factor and pollution load index

To assess the individual rates of trace elements accumulation, about 200 CFs were calculated from the concentrations of Table 1 and the results are listed in Table 2. Across the whole Rouiba–Reghaia region, CFs dramatically varied among assayed elements and sampling sites, being as low as 0.11 for Se at IZ1 while peaking at 893 for Ti at IZ2. Thus, regardless of the sampling zone and according to the classification of Boamponsem et al. (2010) (see 2.4.1), 52% of the studied areas were identified as severely contaminated, 17% exhibited a medium contamination, 14% were weakly polluted, and in only 17% of selected areas contamination was found negligible.

Next, PLIs were calculated from the CFs for further understanding the implication of air pollutants deposition and its repartition between the six selected areas. According to the ranking of 2.4.2 all regions exhibited very high PLIs, ranging from 2.87 at the RNR site to 7.08 at the IZ4 industrial site (Table 2).

A combined examination of CF and PLI values revealed that, despite it is very distant from the main sources of anthropogenic emissions, the RNR area was found strongly polluted by twelve elements, including several metals (Cd, Cu, Cr, Ga, Hg, Ti, V) with only a few elements being recovered at non contaminant levels (i.e., Ba, Fe, Yb, Rb, and Se). Moreover, Br and Hg sampled there afforded the highest CFs as compared to all other sampling sites. The fact that, in the RU zone adjacent to RNR CFs for most elements, particularly for Cu, La, Ce, Tb, Sb, Yb, Rb, and Ti, were found increased, (e.g., being 7- and 140-fold more elevated for Cu and Rb, respectively) may explain why RU showed a higher PLI value (Table 2).

As expected, the four IZ industrial areas resulted in the most elevated PLIs in relation with dramatic increases in the CFs. Hence, the IZ4 site was found the most impacted by air pollution, having CF ≫3 for 21 elements and a PLI ~7 and in this area the lichen contents increases were (times): Rb (123), Sb (63), Ti (4), V (2), Cu (10), Cr 2), Cd (7), and La (33) as compared to RNR. Contrary to these strong metal pollutants, the low CFs for Ba and Se recorded at all sites suggested these elements were unsignificant pollutants in the whole studied region.

### 3.3. Enrichment factor calculations

According to the classification of Xiong et al. (2017), As, Cd, Cu, In, Hf, La, Hg, Zn, Br, Se, Pb, and Ga were moderately to highly enriched in the vast majority of study sites (Table 2), showing their main anthropogenic origin. Noteworthy, highly elevated EFs >350 were found for Sb in RU and IZ sites, peaking at 4167 at IZ3. Regarding EFs even the RNR zone was highly impacted, e.g., by Ga Sb, Se, and Pb.

EFs ≤1 were recorded for Ba and Cr over the whole studied zones, indicating they may originate mainly from soil and crust sources. The class 1 and 2 distribution of EFs for Al, Sc, Rb, Fe, Co, Nd, Sm, Tb, Lu, Sc, Ti, V, Th, U, Ce, Eu, Yb, and Mn suggests that these elements may originate from both natural and artificial sources.

### 3.4. Multivariate analysis

Cluster analysis, used to distinguish between the most polluted sites, allowed to differentiate IZ4 (Cluster 3) from the other IZ1−3 sites (Cluster 2) which showed a similar lower pollution exposure level (Fig. 2B). Unexpectedly, the RU and RNR sites could be grouped into the same less exposed Cluster 1, yet exhibiting a statistically higher contamination than the TH control zone (Cluster 4). This distinction of TH as an outgroup confirmed the consistency of the choice of the Theniet El-Had National Park as a non polluted site. A further CA analysis over all studied sites allowed splitting the pollutants into the most (Al, Fe, Mn, Pb, and Zn; Cluster I), average (e.g., Ti, Cu, and Sb; Cluster II), and less (Cluster III) abundant elements (Fig. 2C).

In order to determine the influence of each element in the classification of the sampling sites, a PCA was performed on the basis of element contents recorded at each site. Despite the narrowness of the regional area of interest limited the number of samples sites vs. the number of assayed elements, the reliability of the PCA remains acceptable enough for a preliminary (Filzmoser and Reimann, 2002). As illustrated in Fig. 3A, the first two principal components PC1 and PC2 accounted for 75% of the total variance recorded in the trace element data set. The PC1 component accounted for 59% of the total variance and was positively correlated with almost all measured elements, except Se which appears negatively correlated while Ba, As, and Br are not correlated. Furthermore, the PLIs, which were plotted as a supplementary variable, were also positively correlated with PC1 (Fig. 3B). Globally, Fig. 3 allowed ranking the global extent of pollution among sites as follows: IZ4 > IZ2 > IZ1 > IZ3 > RU ≥ RNR, a result in accordance with cluster analysis of Fig. 2. Moreover, elements of Cluster I (except Pb) were negatively correlated with PC2, but almost all elements belonging to Clusters II and III were correlated with PC1. In addition to Pb, Cd, Cu, Cr, Ga, Hf, La, Ce, Sm, Hg, Sb, Ti, V, Th, and U (in Clusters II and III; Fig. 2B) were found to account for ~70% of the PC1 computation (Table S4; Supplementary materials), suggesting they are the main air pollutants in the studied area.

The results of MCA are shown in Fig. 4, evidencing that the first two plots (MC1 vs. MC2) accounted for 95% of the total measured correspondence. Among the variables, CF2−EF1; CF3−EF2; CF4−EF3 and to a lesser extent CF4−EF4, and CF4−EF5 appeared clearly associated. Trace elements gathered in Groups 12, 15, and 17 expressed both the highest CFs and EFs (CF class 4 and EF classes 3–5). According to these Groups, the most accumulated and enriched elements in the industrial sites, especially in IZ2,4, were Sb, Zn, Cu, and La, whereas Pb, Ga, and Cd mainly accumulated in both urban and industrial sites.

**Table 1**
Elements concentrations[a] (μg.g$^{-1}$ dw) in thalli of transplanted lichens[b] *Pseudevernia furfuracea* v. *Furfuracea* in the control (TH) and urban-industrial monitoring sites[c].

| Element | TH | | RNR | | RU | | IZ1 | | IZ2 | | IZ3 | | IZ4 | |
|---|---|---|---|---|---|---|---|---|---|---|---|---|---|---|
| | Mean | Min–Max | Mean | Min–Max | Mean | Min–Max | Mean | Min–Max | Mean | Min–Max | Mean | Min–Max | Mean | Min–Max |
| Al | 573 | 548–603 | 921** | 909–930 | 1539*** | 1482–1611 | 1168*** | 987–1270 | 2640*** | 2480–2840 | 1588*** | 1524–1690 | 4396*** | 4328–4470 |
| As | 0.33 | 0.32–0.35 | 0.66** | 0.53–0.79 | 0.98 | 0.69–1.45 | 0.24 | 0.22–0.26 | 0.66 | 0.64–0.68 | 0.24 | 0.19–0.33 | 0.25 | 0.25–0.26 |
| Ba | 6.20 | 5.30–6.70 | 1.28*** | 1.27–1.30 | 1.61*** | 1.22–2.13 | 2.70*** | 2.41–2.85 | 4.47** | 4.21–4.85 | 2.62*** | 2.30–2.80 | 5.68 | 5.52–5.80 |
| Br | 17.5 | 15.5–18.9 | 5.4*** | 4.8–6.1 | 3.2*** | 2.2–4.1 | 18.0 | 16.4–19.5 | 37.8*** | 36.5–38.9 | 15.0 | 12.0–17.0 | 3.2*** | 3.1–3.2 |
| Cd | 0.21 | 0.16–0.25 | 4.90** | 3.85–6.25 | 4.20* | 3.50–5.30 | 6.30** | 5.70–7.20 | 5.80** | 4.90–7.00 | 4.30** | 4.10–4.50 | 31.30*** | 29.4–34.5 |
| Co | 0.23 | 0.20–0.28 | 0.45 | 0.22–0.72 | 0.25 | 0.22–0.32 | 0.31 | 0.25–0.38 | 0.57** | 0.50–0.62 | 0.31 | 0.28–0.35 | 0.39 | 0.37–0.43 |
| Cu | 0.2 | 0.2–0.3 | 6.0 | 5.31–7.01 | 41.2** | 29.9–59.3 | 39.3* | 25.9–57.4 | 41.6** | 38.9–45.3 | 39.6** | 29.4–55.8 | 59.0** | 45–75 |
| Cr | 0.07 | 0.07–0.08 | 1.02** | 0.98–1.05 | 1.29** | 0.96–1.59 | 1.41*** | 1.25–1.52 | 1.67*** | 1.56–1.82 | 1.50*** | 1.37–1.60 | 1.73*** | 1.58–1.89 |
| Cs | 0.15 | 0.15–0.16 | 0.65*** | 0.52–0.76 | 0.88*** | 0.79–0.99 | 0.64*** | 0.61–0.68 | 0.96*** | 0.90–1.02 | 0.14 | 0.14–0.15 | 1.56*** | 1.51–1.60 |
| In | 0.05 | 0.05–0.06 | 0.07 | 0.07–0.08 | 0.05 | 0.05–0.06 | 0.10** | 0.09–0.11 | 0.30*** | 0.27–0.35 | 0.36*** | 0.30–0.41 | 0.05 | 0.05–0.06 |
| Fe | 1031 | 1006–1050 | 670** | 620–675 | 484*** | 390–573 | 2598*** | 2580–2614 | 986 | 887–1059 | 1968*** | 1940–2010 | 2561*** | 2356–2752 |
| Ga | 0.6 | 0.6–0.7 | 50.0*** | 49.0–51.0 | 20.6** | 15.8–25.8 | 10.9 | 9.2–11.9 | 33.0*** | 30.0–36.0 | 12.0 | 10.8–12.7 | 59.5*** | 47–72 |
| Hf | 0.19 | 0.17–0.22 | 0.56*** | 0.54–0.57 | 0.53*** | 0.49–0.57 | 0.65*** | 0.61–0.72 | 0.79*** | 0.76–0.85 | 0.49** | 0.42–0.55 | 0.88*** | 0.76–0.98 |
| La | 0.72 | 0.71–0.75 | 2.50 | 1.72–3.80 | 5.40 | 3.86–7.93 | 50.03** | 29.7–67.8 | 33.60* | 22.5–44.7 | 46.4** | 33.2–66.1 | 71.4*** | 59.7–85 |
| Ce | 1.3 | 0.3–1.9 | 7.6** | 6.3–9.4 | 10.4** | 8.5–12.8 | 9.7** | 8.7–10.4 | 10.9*** | 9.7–11.8 | 8.28** | 6.7–9.4 | 12.5*** | 9.8–16 |
| Nd | 0.98 | 0.92–1.05 | 1.52 | 1.50–1.58 | 1.27 | 1.28–1.43 | 1.20 | 1.18–1.23 | 2.28** | 1.73–2.95 | 2.28** | 1.98–2.54 | 1.96* | 1.40–2.54 |
| Sm | 0.08 | 0.06–0.09 | 0.18** | 0.17–0.19 | 0.14 | 0.08–0.19 | 0.21** | 0.17–0.25 | 0.24*** | 0.22–0.26 | 0.19** | 0.18–0.21 | 0.27*** | 0.25–0.28 |
| Eu | 0.05 | 0.01–0.07 | 0.25 | 0.24–0.26 | 0.06 | 0.03–0.07 | 0.14 | 0.09–0.21 | 0.13 | 0.09–0.15 | 0.35* | 0.09–0.53 | 0.75*** | 0.65–0.85 |
| Tb | 0.01 | 0.01–0.02 | 0.02 | 0.01–0.02 | 0.06* | 0.05–0.07 | 0.07* | 0.05–0.07 | 0.13*** | 0.09–0.18 | 0.06* | 0.05–0.07 | 0.06* | 0.05–0.07 |
| Yb | 0.05 | 0.04–0.06 | 0.04 | 0.03–0.05 | 0.04 | 0.03–0.04 | 0.15 | 0.07–0.24 | 0.16 | 0.08–0.25 | 0.17 | 0.09–0.27 | 0.47* | 0.44–0.50 |
| Lu | 0.01 | 0.01–0.02 | 0.05 | 0.02–0.08 | 0.01 | 0.01–0.02 | 0.07* | 0.06–0.07 | 0.08** | 0.05–0.09 | 0.08* | 0.05–0.14 | 0.08* | 0.06–0.09 |
| Mn | 79 | 60–92 | 119** | 111–125 | 173** | 111–254 | 228** | 220–235 | 250*** | 240–260 | 53 | 49–60 | 181** | 167–201 |
| Hg | 0.03 | 0.03–0.04 | 0.09** | 0.08–0.09 | 0.04 | 0.03–0.04 | 0.05* | 0.02–0.08 | 0.06** | 0.05–0.07 | 0.06** | 0.04–0.09 | 0.06** | 0.03–0.08 |
| Rb | 0.11 | 0.09–0.13 | 0.09 | 0.09–0.10 | 9.43*** | 9.10–9.82 | 0.21** | 0.19–0.21 | 0.09 | 0.09–0.10 | 0.17*** | 0.17–0.18 | 9.40*** | 8.23–10.65 |
| Sb | 0.25 | 0.21–0.30 | 0.32 | 0.28–0.35 | 1.30 | 0.97–1.55 | 7.95 | 2.60–12.85 | 12.03** | 5.59–17.95 | 15.89** | 11.80–20.10 | 20.00*** | 18.5–21.7 |
| Sc | 0.10 | 0.10–0.11 | 0.12 | 0.11–0.13 | 0.18** | 0.15–0.21 | 0.43*** | 0.39–0.46 | 0.37*** | 0.35–0.39 | 0.84*** | 0.83–0.85 | 0.06 | 0.06–0.06 |
| Se | 1.02 | 0.99–1.05 | 0.13*** | 0.12–0.14 | 0.13*** | 0.12–0.13 | 0.12*** | 0.11–0.13 | 0.31*** | 0.30–0.32 | 0.15* | 0.13–0.17 | 0.13* | 0.11–0.15 |
| Pb | 8.0 | 6.5–9.5 | 19.0 | 17.0–20.0 | 31.1 | 25.0–37.9 | 202** | 119–266 | 162** | 136–190 | 253*** | 181–321 | 268*** | 198–350 |
| Ti | 0.2 | 0.1–0.2 | 18.5 | 16.3–21.1 | 53.9** | 45.7–66.3 | 103.0*** | 92.0–115.0 | 134.0*** | 115–154 | 98.6*** | 89–109 | 73*** | 69–80 |
| V | 0.71 | 0.66–0.81 | 6.46 | 3.22–9.61 | 1.68 | 1.02–2.71 | 5.99*** | 2.05–9.21 | 3.14** | 2.84–3.58 | 4.12*** | 1.70–6.96 | 11.86*** | 7.68–15.32 |
| Th | 0.12 | 0.11–0.13 | 0.28 | 0.28–0.29 | 0.27 | 0.26–0.29 | 0.50* | 0.40–0.60 | 0.51** | 0.43–0.61 | 0.79*** | 0.66–0.98 | 0.81*** | 0.71–0.91 |
| U | 0.04 | 0.03–0.04 | 0.09** | 0.05–0.12 | 0.06 | 0.05–0.07 | 0.14 | 0.07–0.18 | 0.13*** | 0.11–0.17 | 0.12 | 0.07–0.17 | 0.15*** | 0.15–0.16 |
| Zn | 37 | 29–42 | 67 | 61–71 | 75* | 70–83 | 78** | 68–93 | 114*** | 98–124 | 44. | 27–59 | 113*** | 93–128 |

[a] Values expressed as means ± standard deviation from three independent determinations performed in duplicate, were obtained by INAA, except for Pb and Cd which were measured by XRF.
[b] Transplanted lichens were exposed for 3 months during the winter period (January–April).
[c] TH, Theniet Elhad; RNR, Reghaia nature reserve; RU, Reghaia urban site; IZ1−4, Rouiba−Reghaia industrial zones. Significance (ANOVA followed by Dunnett's test) vs. values at TH site: *$P < 0.5$, **$P < 0.01$, and ***$P < 0.001$.

**Table 2**
Contamination factor (CF), enrichment factor (EF), and pollution load index (PLI) calculated[a] from the trace elements concentrations accumulated in the transplanted lichens *Pseudevernia furfuracea* at study sites[b].

| Element | RNR | | RU | | IZ1 | | IZ2 | | IZ3 | | IZ4 | |
|---|---|---|---|---|---|---|---|---|---|---|---|---|
| | CF | EF | CF | EF | CF | EF | CF | EF | CF | EF | CF | EF |
| Al | 1.6 | 0.8 | 2.7 | 1.6 | 2.0 | 0.3 | 4.6 | 1.8 | 2.7 | 0.6 | 7.6 | 1.7 |
| As | 1.9 | 32.8 | 2.9 | 22.7 | 0.7 | 9.3 | 2.0 | 11.4 | 0.7 | 4.1 | 0.7 | 2.7 |
| Ba | 0.2 | 0.3 | 0.2 | 0.2 | 0.4 | 0.5 | 0.7 | 0.3 | 0.4 | 0.3 | 0.9 | 0.3 |
| Br | 12.0 | 203 | 0.2 | 67 | 1.0 | 531 | 2.2 | 493 | 0.9 | 325 | 0.2 | 24.7 |
| Cd | 23.0 | 22.5 | 19.7 | 15.0 | 29.5 | 29.9 | 27.2 | 12.2 | 20.2 | 15.0 | 147 | 39.4 |
| Co | 1.9 | 1.6 | 1.1 | 0.5 | 1.3 | 0.9 | 2.5 | 0.7 | 1.3 | 0.6 | 1.7 | 0.3 |
| Cu | 28 | 5.3 | 187 | 3.7 | 179 | 50.3 | 189 | 21.5 | 180 | 34.3 | 270 | 18.5 |
| Cr | 14.5 | 0.9 | 18.2 | 0.7 | 19.9 | 1.0 | 23.6 | 0.5 | 21.0 | 0.8 | 24.3 | 0.3 |
| Cs | 4.2 | 19.4 | 5.7 | 15.8 | 4.2 | 15.0 | 6.3 | 10.0 | 0.5 | 1.2 | 10.1 | 9.7 |
| In | 1.4 | 26.6 | 1.0 | 5.4 | 1.9 | 29.6 | 6.0 | 38.3 | 7.2 | 75.5 | 1.0 | 1.9 |
| Fe | 0.6 | 1.0 | 0.5 | 0.5 | 2.5 | 3.2 | 1.0 | 0.5 | 1.9 | 0.8 | 2.4 | 0.9 |
| Ga | 79 | 2347 | 32 | 578 | 17 | 405 | 52 | 543 | 19 | 328 | 94 | 588 |
| Hf | 2.9 | 16.6 | 2.8 | 9.5 | 3.4 | 15.4 | 4.1 | 8.2 | 2.5 | 8.5 | 4.6 | 5.5 |
| La | 3.4 | 5.7 | 7.4 | 7.4 | 68.9 | 90.5 | 46.2 | 26.9 | 63.9 | 61.8 | 98.3 | 34.3 |
| Ce | 5.8 | 10.2 | 8.0 | 8.3 | 7.4 | 10.2 | 8.3 | 5.1 | 6.3 | 6.4 | 9.6 | 3.5 |
| Nd | 1.5 | 3.3 | 1.2 | 1.6 | 1.2 | 2.0 | 2.3 | 1.7 | 2.3 | 2.8 | 2.0 | 0.8 |
| Sm | 2.2 | 2.3 | 1.7 | 1.0 | 2.6 | 2.1 | 3.0 | 1.0 | 2.4 | 1.5 | 3.3 | 0.7 |
| Eu | 4.9 | 11.3 | 1.1 | 1.5 | 2.7 | 4.9 | 2.4 | 2.0 | 6.9 | 9.2 | 14.6 | 7.0 |
| Tb | 1.5 | 1.6 | 4.6 | 2.9 | 4.8 | 4.0 | 9.0 | 3.3 | 4.5 | 2.7 | 4.5 | 1.0 |
| Yb | 0.6 | 0.8 | 2.6 | 0.5 | 3.0 | 3.3 | 3.2 | 1.6 | 3.3 | 2.7 | 9.3 | 2.7 |
| Lu | 2.8 | 3.7 | 0.7 | 0.9 | 4.1 | 6.5 | 4.4 | 3.0 | 4.9 | 5.6 | 4.5 | 1.9 |
| Mn | 1.5 | 11.8 | 2.1 | 10.2 | 2.8 | 17.0 | 3.1 | 8.6 | 0.7 | 3.0 | 2.3 | 3.7 |
| Hg | 3.0 | 99.8 | 1.3 | 18.8 | 1.6 | 48.0 | 1.8 | 24.0 | 1.9 | 46.0 | 1.8 | 13.6 |
| Rb | 0.7 | 1.0 | 85.7 | 6.1 | 1.9 | 0.2 | 0.9 | 0.4 | 1.5 | 0.1 | 85.6 | 2.1 |
| Sc | 1.2 | 0.5 | 1.8 | 0.5 | 4.1 | 1.3 | 3.6 | 0.5 | 8.2 | 2.0 | 0.6 | 0.1 |
| Se | 0.1 | 238.3 | 0.1 | 137.5 | 0.1 | 171.9 | 0.3 | 196.2 | 0.2 | 93.8 | 0.1 | 47.9 |
| Pb | 2.4 | 118 | 3.9 | 119 | 25.3 | 102 | 20.2 | 361 | 31.6 | 93 | 33.5 | 359 |
| Ti | 123 | 0.3 | 359 | 0.6 | 686 | 1.3 | 893 | 0.7 | 653 | 0.9 | 486 | 0.2 |
| V | 9.0 | 5.0 | 2.4 | 0.8 | 8.4 | 3.7 | 4.4 | 0.8 | 5.8 | 1.9 | 16.7 | 1.9 |
| Th | 2.3 | 2.6 | 2.3 | 1.5 | 4.2 | 3.7 | 4.3 | 1.7 | 6.5 | 4.3 | 6.8 | 1.6 |
| U | 2.3 | 3.1 | 1.7 | 1.3 | 3.4 | 3.6 | 3.3 | 1.6 | 2.8 | 2.2 | 3.8 | 1.0 |
| Zn | 1.8 | 84.9 | 2.0 | 60.0 | 2.1 | 78.5 | 3.0 | 50.8 | 1.1 | 32.6 | 3.0 | 30.4 |
| **PLI index** | 2.87 | | 3.18 | | 4.68 | | 5.86 | | 4.61 | | 7.08 | |

CF indicator: CF $<$ 1.2, no contamination, 1.2 = CF $<$ 2, light contamination, 2 = CF $<$ 3, medium contamination, and CF $\geq$ 3, heavy contamination.
EF indicator: EF $\leq$ 1, rarely enriched (soil and crust source); 1$<$ EF $\leq$ 10, mildly enriched (natural and artificial sources); 10$<$ EF $\leq$ 100, moderately enriched (artificial sources); 100$<$ EF $\leq$ 1000, highly enriched; EF $>$ 1000, extremely enriched.
PLI indicator: PLI $<$0.9, no pollution; 1 $\pm$ 0.1, background level; 1.1 $<$ PLI $<$1.5, low pollution; 1.5 = PLI $<$2.0, moderate pollution; 2.0 = PLI $<$2.5, high pollution; PLI $\geq$2.5, very high pollution.
[a] CF, EF and PLI indexes were calculated as indicated in the methods section. For each element at the TH control site, CF, EF and PLI values of 1 are taken as the background level. Ranges of CF, EF and PLI values were respectively categorized into the following contamination classes.
[b] RNR, Reghaia nature reserve; RU, Reghaia urban site; IZ1−4, Rouiba−Reghaia industrial zones.

## 4. Discussion

### 4.1. Bioaccumulation of trace elements

It was not unexpected that heavy metals and rare earths concentrations in *Pseudevernia furfuracea* lichen transplants are significantly higher in all selected urban-industrial sites of Rouiba−Reghaia region relative to the Reghaia Nature Reserve and the Theniet El-Had control site. In this latter regard, background elements concentrations found at the TH site are plausible control levels (Bergamaschi et al., 2004; Ancora et al., 2021) in agreement with the literature values obtained in unpolluted sites worldwide listed in Table S5 (Freitas et al., 1993; Adamo et al., 2003; Culicov and Yurukova, 2006; Malaspina et al., 2014; Pantelica et al., 2016). Indeed, lichen biomonitoring studies, including the present investigation, have identified Al, Fe, and, in a lesser extent, Mn and Zn, as the major contributors to the contemporary background atmospheric burden.

The amounts of recovered elements over a sampling area depend on several factors, including the nature, the distance, and the strength of the pollution sources (Bozkurt, 2017), the lichen species and its bioaccumulation ability, and the accurate analytical methods used. Table 3 allows comparison of the average concentrations of airborne elements for the whole Rouiba−Reghaia region with comparable biomonitoring surveys in urbanized areas of Bosnia Herzegovina (Humerovic et al., 2015), The Netherlands (de Bruin, 1990), Brazil (Saiki et al., 1997), China (Zhao et al., 2019), France (Ratier et al., 2018), and Italy (Adamo et al., 2003; Frati et al., 2005; Malaspina et al., 2014). Besides the fact that still Al and Fe remained the most dominant pollutants, followed by significant contributions of Cu, Pb, Mn, Ti, and Zn, the present study also pinpointed at Pb, Cd, Sb, and Cu as unusually strong atmospheric pollutants as compared to other regions wordwide, and at Ba, Cr, Sc, Se and U as relatively low contaminants. Strikingly, La levels were significantly higher in the Rouiba−Reghaia region (2- to 25-fold; see Table 3), a worrisome concern owing to the emergence of pollution by rare earths (Zhao et al., 2019).

### 4.2. Sites classification

Perhaps the most important result of this study is that, although the RNR and RU areas have similar lithological features and their average distance from the strongly polluted industrial IZ4 site is only 13 km and 20 km, respectively, they belong to the same Cluster 1 based on CA (Fig. 2B) and high PLIs (Table 2), yet RNR retained the lowest overall contamination level (Table 1). These data can help advocate for saving urban forests and/or enhancing large green spaces installation for providing barriers against airborne pollutants that are intensively

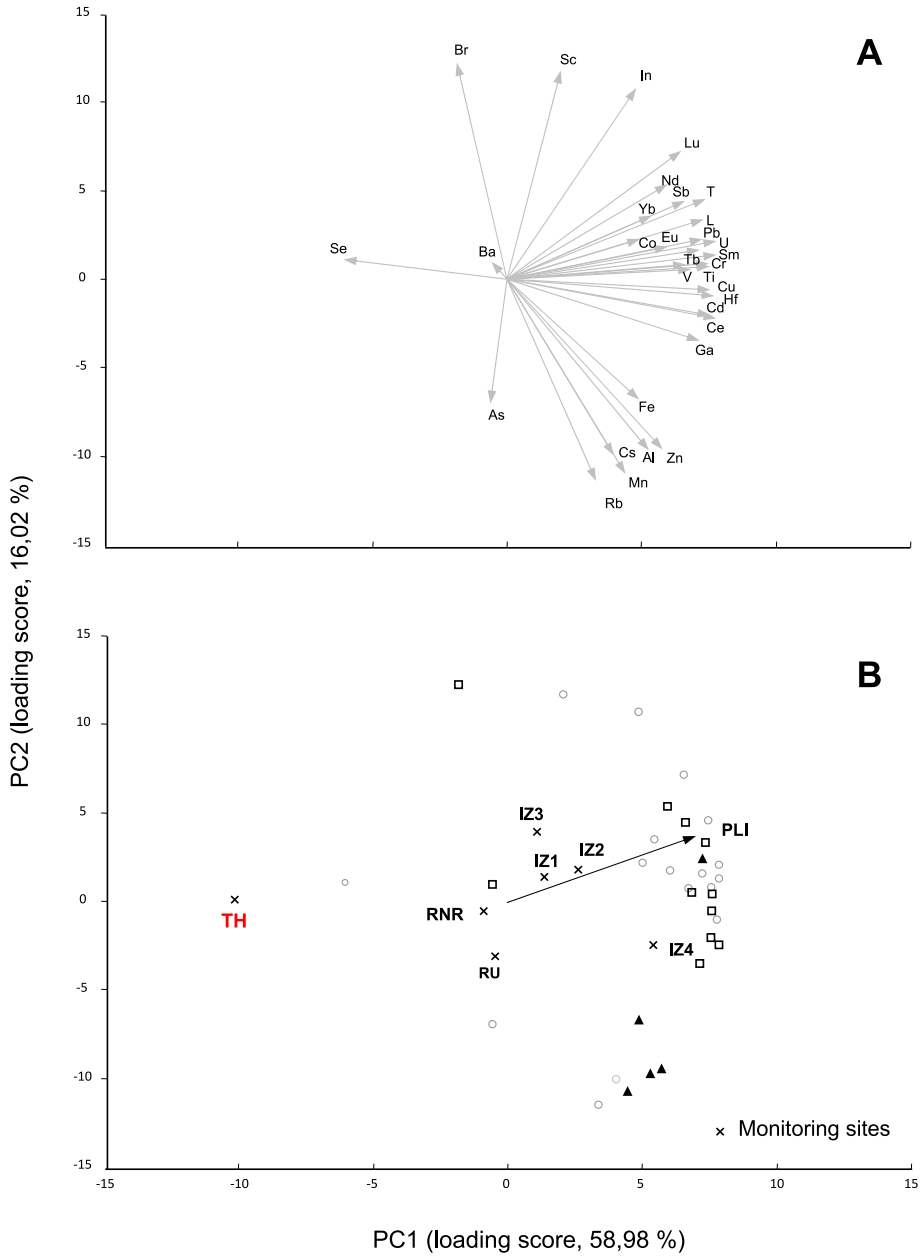


**Fig. 3.** Principal component analysis biplot (PC1 vs. PC2) of elements in lichens at the each monitoring site. A) Loading vectors of elements. B) Elements were symbolized according to the three main Clusters I (▲), II (□), and III (○) resulting from cluster analysis of Fig. 2C and monitoring sites plot. Pollution load index (PLI; black arrow) is also plotted as a supplementary variable.

spreading from the industrial zones to the rural and urban areas. In this regard, recent approaches were proposed for modeling the air mitigation potential of urban vegetation (Baraldi et al., 2019; Contardo et al., 2020). Since there is sparse vegetation around the RU site (Fig. 1C), air pollution in this area reflects the high railway and road traffics and prevailing winds carrying air particles and soil dusts from one area to another.

Cluster analysis (Fig. 2B) discriminated the more Eastern of the studied industrial sites, IZ4, in a single most dramatically contaminated Cluster 3. Indeed, compared to the traffic (e.g., roadside dust) and industrial (i.e., pipes manufactures and gas processing) pollution determinants of the even more Eastern RU zone, atmospheric contamination at IZ4 may be amplified by emissions from a steel melting plant (EPE Rouiba Foundries) and would not benefit from the 'protective' effect of the RNR area discussed above. Multivariate analysis resulted in a common Cluster 2 for the other IZ1−3 industrial sites which can be considered having a similar poor air quality. Intriguingly, in Cluster 2 PLIs were found decreasing moving westward, i.e., IZ1 ~ IZ3 < IZ2 (Table 2), seemingly not associated to the prevalent dominant winds from the east in the region. Lastly, the TH control site considered as a relatively clean area, has been included in Group 4.

Arguably, the most probable common aerial elemental sources in IZ1−4 area could be vehicle emissions in the case of Ti, Cu, Sb, and Sn, and industrial activities for Al, Fe, Mn, and Cd (Bajpai and Upreti, 2012; Lucadamo et al., 2016; Ratier et al., 2018). This is consistent with CA and PCA calculations (Fig. 3B) indicating that highly bioaccumulable elements in lichens were found at IZ1−4 sites from several potential sources. The overall consistency between CA and PCA indexes may imply that the clustering of sample sites in the present study was done in a rather convincing pattern (Boamponsem et al., 2017).

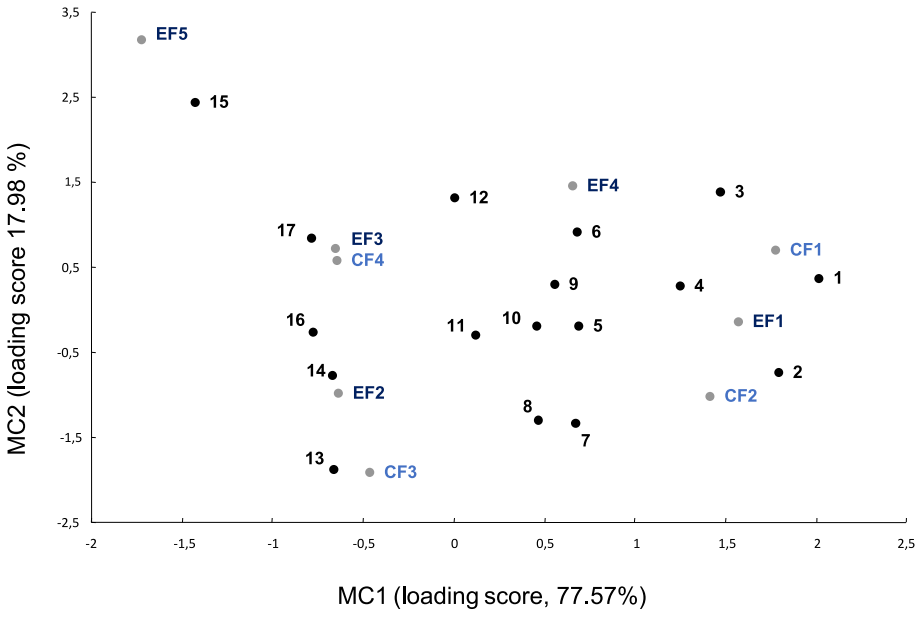


**Fig. 4.** Multiple correspondence analysis biplot (MC1 vs. MC2) of elements and their corresponding classes of contamination factor (CF)−enrichment factor (EF) at monitoring sites The considered classes were: CF1 (CF class 1): CF < 1.2, no contamination; CF2 (CF class 2): 1.2 = CF < 2, light contamination; CF3 (CF class 3): 2 = CF < 3, medium contamination; CF4 (CF class 4): CF ≥ 3, heavy contamination; EF class 1 (EF1): EF ≤ 1, rarely enriched (soil and crust source); EF class 2 (EF2): 1 < EF ≤ 10, mildly enriched (natural and artificial sources); EF class 3 (EF3): 10 < EF ≤ 100, moderately enriched (artificial sources); EF class 4 (EF4): 100 < EF ≤ 1000, highly enriched; EF class 5 (EF5): EF > 1000, extremely enriched. Numerals with boldface (1–17) refer to chemical elements monitored in the considered sites (indicated between hooks) that obtained similar MCA plotting scores as follow: 1 (CF1−EF1): Ba [IZ1−4, IZ3, RU, RNR], Co [RU], Fe [IZ2, RU, RNR], Lu [RU], Rb [IZ2, RNR], Sc [IZ4, RNR], Yb [RNR]; 2 (CF2−EF1): Al [RNR], Co [IZ1, IZ3,4], Fe [IZ3], Nd [IZ4], Rb [IZ1,3], Sc [RU], Sm [RU]; 3 (CF1−EF4): Br [IZ1,3], Sb [RNR], Se [RNR, RU, IZ1,2]; 4 (CF2−EF4): Sb [RNR]; 5 (CF1−EF2): As [IZ1,3,4], Br [RU, IZ4], Cs [IZ3], Eu [RU], Mn [IZ3], In [RU, IZ4]; 6 (CF1−EF3): Se [IZ3,4], Zn [IZ3]; 7 (CF3−EF1): Al [IZ1,3], Co [IZ2], Fe [IZ4], V [RU], Yb [RU]; 8 (CF2−EF2): Co [RNR], Nd [RNR, RU, IZ1], Tb [RNR], U [RU]; 9 (CF4−EF1): Cr [RNR, RU, IZ1−4], Sc [IZ2], Sm [IZ2,4], Tb [IZ4], Ti [RNR, RU, IZ2−4], U [IZ4], V [IZ2]; 10 (CF2−EF3): As [RNR], Mn [RNR], Zn [RNR], In [RNR, IZ1]; Hg [RU, IZ1−4]; 11 (CF3−EF4): Br [IZ2], Pb [RNR]; 12 (CF4−EF4): Br [RNR], Ga [RU, IZ1−4], Pb [RU, IZ1,2,4], Sb [RU]; 13 (CF3−EF2): Al [RU], Eu [IZ1, IZ2], Fe [IZ1], Hf [RU, IZ3], Lu [RNR], Mn [IZ4], Nd [IZ2,3], Sm [RNR, IZ1,3], Th [RNR, RU], U [RNR, IZ3]; 14 (CF3−EF4): As [RU, IZ2], Hf [RNR], Mn [RU, IZ1], Zn [RU,IZ1]; 15 (CF4−EF5): Ga [RNR], Sb [IZ1−4]; 16 (CF4−EF2): Al [IZ2, IZ4], Ce [RU, IZ2−4], Cs [IZ2,4], Cu [RNR, RU], Eu [IZ3,4], Hf [IZ2,4], La [RNR, RU], Lu [IZ1−4], Mn [IZ2], Rb [RU, IZ4], Sc [IZ1, IZ3], Tb [RU, IZ1−3], Th [IZ1−4], Ti [IZ1], U [IZ1,2], V [RNR, IZ1,3,4], Yb [IZ1−4]; 17 (CF4−EF3): Cd [RNR, RU, IZ1−4], Ce [RNR, IZ1], Cs [RNR, RU, IZ1], Cu [IZ1−4], Eu [RNR], Hf [IZ1], Hg [RNR], In [IZ2,3], La [IZ1−4], Pb [IZ3], Zn [IZ2,4].

### 4.3. Trace element sources identification

Both natural and anthropogenic emissions contribute locally to atmospheric trace elements enrichment and deposition. If grouping statistical methods permits establishing high correlations for particular elements in regional clusters to point out common specific local emitters (Boamponsem et al., 2010; Demiray et al., 2012), such identification is rather complex in practice because some of the elements can be emitted from several sources. Indeed, Cluster I elements discriminated by CA (Fig. 2C), mostly lithogenic (Agnan et al., 2015; Paoli et al., 2015), may also derive from anthropogenic sources such as road traffic, while the variability seen in Clusters II and III (this latter including Co, As, Th, Hf, Cs, Cr, Rb, Se, Sc, U, Sm, Eu, Yb, Lu, Tb, Hg, and In) mainly reflects noticeable anthropogenic industrial and agricultural activities.

PCA, a convenient statistical tool for exploring significant contamination sources in air, soil or water (Sorbo et al., 2008; Boamponsem et al., 2010; Zeng et al., 2015; Boonpeng et al., 2017), yielded a PC1 component (Fig. 3A) predominantly correlated with 16 bioaccumulated elements (i.e., Cd, Cu, Cr, Pb, Ga, La, Ti, Ce, HF, Sm, Tb, Hg, Sb, V, U, and Th), being largely associated with industrial and vehicle emissions, and concentrating in the areas adjacent to high road traffic (Boamponsem et al., 2010; Aslan et al., 2013; Contardo et al., 2020). Some elements from Clusters III (As, Sc, In, Rb, Cs, Lu) and I (Al, Fe, Mn, Zn) as well as Br were negatively correlated with the PC2 component and displayed high loadings, representing 16% of the total variance of the data set (Table S4; Supplementary materials). This factor could likely be constituted by a mixture of airborne elements arising from terrestrial, marine and industrial pollution (Incerti et al., 2017).

### 4.4. Accessing a general typology of air pollution in the Rouiba–Reghaia region

The data of MCA analysis are discussed below for selected groups of contamination patterns defined in Fig. 4.

The highest contamination score in Group 15 (CF4−EF5) reflects an extreme bioaccumulation of Sb and Ga in all IZ sites and RNR, respectively. MCA high score in Group 12 (CF4−EF4) indicated that these metals, together with Pb are also located at high levels (CF ≥ 3) in all industrial sites (except for Pb at IZ3), while Sb dominated in RU. The rise in Ga pollution seen here could be related to its increasing use in electronics manufacturing (arsenide and nitride derivatives are used in integrated circuits, optoelectronic devices, photodetectors, and solar cells) and nuclear medicine. However, still Ga environmental impact has not been adequately documented (White and Shine, 2016).

High concentrations of Sb and Pb found in this study are usually observed in the vicinity of oil refineries and chemical plants (Bajpai and Upreti, 2012; Lucadamo et al., 2016; Ratier et al., 2018). Also, these heavy metals are typically traffic-related pollutants, being emitted by fossil fuel combustion, tire and brake linings deterioration, vehicle component wearing, corrosion, lubricating oils or fuel additives (Lough et al., 2005; Fujiwara et al., 2011; Olowoyo et al., 2011; Gianini et al., 2012; Dong et al., 2017; Contardo et al., 2020; Parviainen et al., 2020). The high levels of Sb found in IZ sites and RU may originate from industrial sources metal melting and refining, waste combustion (Bergamaschi et al., 2004) or purification processes (Pacyna and Pacyna, 2001).

An earlier lichen biomonitoring survey of Pb contamination in the Algiers region, where the number of motor vehicles, often old and poorly maintained engines, has exceeded 1.4 million and current regulation for tetraethyl lead content allowance is as high as 0.6 g/L, identified road traffic as the main source of atmospheric Pb pollution (Rahali, 2002). Over the past two decades, this situation was getting worse in the Rouiba–Reghaia region where increased traffic congestion is contributing to an uncontrollable increase in Pb emissions (Bouhila et al., 2015) and it is noteworthy that Algeria was the last country to ban leaded gasoline in 2021. Therefore, because elevated traffic-related

**Table 3**
Elements concentrations ($\mu g.g^{-1}dw$) in thalli of various lichens transplanted in several industrial and urban sites worldwide.

| Element | This work, Algeria[a] | Sao Paulo, Brazil[b] | Jesi, Italy[c] | Sarajevo, Bosnia Herzegovina[d] | Netherlands[e] | Naples, Italy[f] | Genoa, Italy[g] | Fos−sur−Mer, France[h] | Hebei, China[i] |
|---|---|---|---|---|---|---|---|---|---|
| Al | 2042 ± 1219 | 7129 ± 137 | 628 ± 89.5 | – | 5800 (230–21,000) | 1969 | 820 ± 120 | 3661 ± 1554 | 8971 (3561–14,024) |
| As | 0.5 ± 0.32 | 1.057 ± 14 | 0.35 ± 0.03 | 1.76 ± 0.08 | 5.7 (0.5–17) | 0.60 | – | 2.39 ± 1.12 | – |
| Ba | 3.06 ± 1.6 | – | 12.2 ± 1.42 | 28.6 ± 1.2 | – | – | 21.9 ± 6.5 | – | 82.9 (42.7–186.7) |
| Br | 13.76 ± 12.5 | 24.85 ± 0.05 | – | 10 ± 0.4 | 56 (15–170) | – | – | – | – |
| Cd | 9.46 ± 10 | 3917 ± 209 | 0.12 ± 0.01 | 0.53 ± 0.08 | 2.8 (0.6–21) | 1.36 | 0.12 ± 0.01 | 0.48 ± 0.24 | 1.43 (0.83–2.3) |
| Co | 0.38 ± 0.1 | 1063 ± 4 | 0.29 ± 0.11 | 0.62 ± 0.03 | 2 (0.2–6.3) | 2.76 | 0,54 ± 0.09 | 1.24 ± 0.42 | 1.81 (1.31–2.89 |
| Cu | 37.87 ± 19 | – | 10.5 ± 2.04 | > 6 | 33 (1.4–120) | 29.6 | 38 ± 53 | 17.9 ± 11.1 | 14.73 (8.36–32.3) |
| Cr | 1.4 ± 0.2 | 16.4 ± 0.1 | 1.88 ± 0.36 | 8.32 ± 0.33 | 26 (4–270) | 4.49 | 6.4 ± 0.9 | 30.0 ± 16.6 | – |
| Cs | 0.75 ± 0.4 | 1016 ± 10 | 0.08 ± 0.01 | 0.45 ± 0.02 | 0.8 (0.2–5) | – | – | – | 1.89 (1.17–2.81) |
| In | 0.14 ± 0.1 | – | – | > 0.2 | – | – | – | – | – |
| Fe | 1544 ± 897 | 4135 ± 21 | 575 ± 49.9 | 1630 ± 65 | 5800 (720–30,000) | 1423 | 820 ± 220 | 14.11 ± 11.78 | 6542 (3446–10,146) |
| Ga | 31 ± 19 | – | 0.17 ± 0.03 | 0.74 ± 0.08 | 47 (2.3–180) | – | – | – | – |
| Hf | 0.65 ± 0.15 | 1464 ± 5 | – | 0.258 ± 0.01 | 1.4 (0.09–8) | – | – | – | – |
| La | 34.9 ± 2.7 | 7.05 ± 0.05 | – | 1.4 ± 0.06 | 6.2 (0.8–35) | – | – | – | 19.06 (13.1–33.3) |
| Ce | 9.9 ± 2.1 | 16.58 ± 0.04 | – | 3.02 ± 0.16 | – | – | – | – | – |
| Nd | 1.75 ± 0.50 | – | – | 1.35 ± 0.07 | – | – | – | – | – |
| Sm | 0.20 ± 0.05 | 1055 ± 1 | – | 0.3 ± 0.01 | – | – | – | – | 2.4 (1.76–3.94) |
| Eu | 0.27 ± 0.2 | 181 ± 2 | – | 0.060 ± 0.006 | – | – | – | – | – |
| Tb | 0.067 ± 0.03 | 103 ± 3 | – | 0.037 ± 0.002 | – | – | – | – | 0.30 (0.20–0.46) |
| Yb | 0.17 ± 0.16 | 346.6 ± 6.7 | – | 0.122 ± 0.006 | 0.4 (0.078–3) | – | – | – | – |
| Lu | 0.064 ± 0.03 | 60.1 ± 0.5 | – | – | 0.071 (0.001–0.46) | – | – | – | – |
| Mn | 167 ± 72 | 164.4 ± 1.2 | 51.1 ± 6.52 | – | 110 (16–400) | 64.5 | 84 ± 27 | 194 ± 116.7 | 124.5 (59.4–242.4) |
| Hg | 0.062 ± 0.02 | – | – | – | 0.5 (0.1–36) | – | – | – | – |
| Rb | 4.40 ± 3.9 | 20.2 ± 0.2 | 3.27 ± 0.66 | 7.71 ± 0.31 | 13 (1.8–62) | – | – | – | 17.72 (11.35–24.34) |
| Sb | 9.59 ± 8 | 2000 ± 10 | – | 0.5 ± 0.03 | 3.3 (0.3–12) | – | – | 1.71 ± 0.61 | 1 (0.64–2.17) |
| Sc | 0.33 ± 0.26 | 1190 ± 3 | – | 0.52 ± 0.03 | 1.1 (0.16–5.2) | – | – | – | – |
| Se | 0.163 ± 0.07 | 665 ± 24 | 0.37 ± 0.38 | 0.169 ± 0.012 | 1.8 (0.4–7.5) | – | – | – | – |
| Pb | 155.95 ± 111 | – | 4.91 ± 0.98 | – | 150 (3.1–370) | 152 | 5.9 ± 3.2 | 21.4 ± 9.4 | 172.8 (55.3–271.1) |
| Ti | 80.18 ± 39 | 510 ± 89 | 0.01 ± 0.00 | – | – | 39.07 | – | – | 433.2 (272–614) |
| V | 5.54 ± 4 | 190.2 ± 8.7 | 1.71 ± 0.15 | – | 32 (5.7–99) | 5.41 | 3 ± 1.2 | 11.7 ± 4.4 | 17.08 (9.35–26) |
| Th | 0.53 ± 0.2 | – | – | 0.41 ± 0.02 | 1.2 (0.14–8.9) | – | – | – | 2.37 (1.14–3.41) |
| U | 0.118 ± 0.03 | – | 0.19 ± 0.02 | 0.145 ± 0.007 | 0.57 (0.09–2.7) | – | – | – | – |
| Zn | 81.9 ± 28.0 | 145.7 ± 0.5 | 40.8 ± 33.2 | 88.9 ± 3.6 | 210 (61–1100) | 243.3 | 69 ± 19 | 70.9 ± 49.6 | 121.2 (61–241.3) |

[a] *Pseudevernia furfuracea* (L.) Zopft, transplanted for 3 months during the winter season in the Rouiba−Reghaia region. For each element, data are expressed as the average of 3 independent values (means ± standard deviation) recorded in the 6 monitoring sites of the Rouiba−Reghaia region (RNR, RU and IZ1−4).
[b] *Canoparmelia texana* (Saiki et al., 1997).
[c] *Evernia prunastri*, transplanted for three months (Frati et al., 2005).
[d] *Hypogymnia physodes* sampled in situ (Humerovic et al., 2015).
[e] *Parmelia sulcata*, sampled in situ (de Bruin, 1990).
[f] *Pseudevernia furfuracea* transplanted for four months (Adamo et al., 2003).
[g] *Pseudevernia furfuracea* transplanted for one month (Malaspina et al., 2014).
[h] *Xanthoria parietina* in situ (Ratier et al., 2018).
[i] *Rhizoplaca chrysoleuca* transplanted for twelve months (Zhao et al., 2019).

atmospheric Pb emissions were still occurring at the time of the present study, it was speculated the substantial contamination levels shown in Table 1 would arise mostly from vehicular traffic.

For many years, the use of leaded gasoline in Europe was assumed as the main source for airborne Pb concentrations, making this metal a reliable indicator for road traffic-related airbone pollution (Zechmeister et al., 2005). In the 1990s, lead-free gasoline was made compulsory in European countries and many studies documented a significant decrease of airborne lead pollution (Loppi and Corsini, 2003; Loppi et al., 2004) and later investigations confirmed that Pb levels in lichens did not correlate anymore with any current road traffic (Paoli et al., 2013). Strikingly, Rola and Osyczka (2019) reported that despite the cessation of leaded fuel commercialization, lead still remains the most prevalent heavy metal in local urban environment likely due to its lengthy residence time and resuspension in roads and urban soils, but also in house dust and domestic heating systems (Loppi and Corsini, 2003; Levin et al., 2021). To sum up, *P. furfuracea* transplants, known to be particularly adapted as Pb biomonitors (Sorbo et al., 2008; Guidotti et al., 2009), may ideally report on possible changes in the atmosphere of Rouiba−Reghaia region consecutive to the current use of unleaded gasoline.

The pollution patterns of Group 17 (CF4−EF3) including Cd, Cu, Hg, and In imply these elements to arose predominantly from artificial sources. High accumulation was found in all monitoring sites for Cd, while Cu, Hg, and In were mostly seen in industrial sites, RNR, and IZ2,3, respectively. Despite its low crustal abundance Cd is widely used in industrial processes, e.g., phosphate fertilizers or anticorrosive agents for manufacturing Ni–Cd batteries. Other sources of Cd emissions include fossil fuels from traffic pollution, emissions from petroleum metallurgical facilities, electroplating, and polyvinyl chloride plastics (see, e.g., Scerbo et al., 2002).

In addition to typical sources of Hg pollution such as steel mills, cement plants, electronics and agrochemical industries (Scerbo et al., 2002; Demiray et al., 2012; Boonpeng et al., 2017), this gaseous and aerosol pollutant is known to be released from contaminated soils and water (López Berdonces et al., 2017; Perez Catán et al., 2020), presumably here in RNR by the polluted lake of Reghaia or the sea.

The anthropogenic origin of In contamination at IZ2,3 sites drawn from its high CFs (Table 2) is consistent with its use as tracer of melting and waste burning (Bruinen de Bruin et al., 2006) or in the production of LEDs and high-efficiency photovoltaic cells (White and Shine, 2016).

Last element of Group 17 examined, Cu, which exhibited extremely high CFs that increased by 7- to 10-fold in RU and IZ4 as compared to TH, respectively, is a typical contaminant (Boamponsem et al., 2010; Aslan et al., 2013; Contardo et al., 2020) associated to road traffic, agricultural practices (use of pesticides and fertilizers) or waste incineration, a common usage at Oued Smar landfill (only ~28 km away from

IZ1 site; Fig. 1B). Lichens biomonitoring is a particularly efficient technique for assessing urban Cu emissions (Vannini et al., 2019). The trends found here for Cu and other Group 17 elements are in accordance with recent reports in similar urban and industrial sites (see, e.g., Agnan et al., 2013).

In Group 14 (CF3−EF4), a high enrichment was found for Zn and Mn at IZ1and RU, and for As at IZ2 and RU. Presumably, high contamination at IZ1 by Zn, a typical indicator for waste incineration, may have the same origin as that by Cu discussed above. In the urban area, Zn may also derive from motor vehicle traffic through the consumption of greasing oils (Boamponsem et al., 2017). Airborne Mn, an abundant and essential micronutrient used in fertilizers and manure, has been shown to induce neurotoxicity upon chronic inhalation of high doses (Kim et al., 2022). Last, bioaccumulation of As found in transplanted lichens appears consistent with known association to fuel combustion (Agnan et al., 2015), steelwork (Demiray et al., 2012), and areas of agriculture production (Pacyna and Pacyna, 2001; Zhou et al., 2018).

Among elements gathered in Group 16 (CF4−EF2), Lu, Th, and Yb were heavily accumulated but mildly enriched at all the IZ sites. Moreover, V, which was also found at RNR, is an environmental marker of vehicle exhaust (Giampaoli et al., 2016), being present in fuel oils, crude petroleum, coal, and is a common component of oil refinery catalysts (Adamo et al., 2003; Brunialti and Frati, 2007). As in Groups 17 and 14 discussed above, the infrastructures surrounding all studied sites, including RNR, may largely contribute to atmospheric metal pollution, a feature described in many other regions worldwide with high traffic and refinery activities (Enamorado-Báez et al., 2015; Zhao et al., 2019).

Conceivably, long distance emissions could contribute to even increase the intrinsic pollution within the Rouiba–Reghaia region. Among such potential 'foreign' metal emitters are the huge Sidi Rezine oil refinery, the Oued Smar industrial zone, and the Meftah cement factory. Also, frequent and strong southern Saharian winds in the region are natural carriers of main road (NR5,11, A1) dusts and rare earths.

Uptake of Al by lichens, which exhibited rare enrichment with low to medium contamination at RNR in Groups 2 (CF2−EF1) and 7 at IZ1,3 (CF3−EF1) sites, showed mild enrichment with heavy contamination in Group 16 at IZ2 (CF4−EF2). This element has a known mixed anthropogenic/natural origin (Agnan et al., 2015), e.g., it can accumulate in lichens due to the erosive action of the winds (Adamo et al., 2003) strongly blowing in the studied region or consecutive to airborne soils dust deposition (Paoli et al., 2015).

Of interest, high CFs and EFs were observed for Br in RNR (scoring at CF4−EF4 in Group 12) and TH sites. In addition to its known industrial uses (fire retardants, water treatments, dyes, pharmaceuticals, pesticides), bodies of water can represent major natural sources of Br. (Bergamaschi et al., 2004).

Finally, while some heavy metals fortunately showed rather low (Fe, Rb, Sc, Sm, Co) or negligible (Ba) EFs and CFs, the scores for Cr and Ti indicated strong contamination but rare enrichment, suggesting a marginal contribution of anthropogenic emissions.

## 5. Conclusions

The findings in this study illustrate the accuracy of the information gained by biomonitoring methods combined to discriminant analysis of contaminated areas. To the authors' knowledge, this is the first comprehensive investigation (33 trace elements measured) of airborne metal pollution in Rouiba−Reghaia, one of the largest, most populated, and highly expanding urban−industrial and agricultural regions in Algeria. This was obtained by application of the transplant technique using the lichen *Pseudevernia furfuracea* which demonstrated outstanding accumulator properties, allowing detection of trace metal concentrations by XRF and INAA within only 3 months of exposure. Of the seven studied sites (comprising the unpolluted TH area) having quite different degrees of industrialization and urbanization the highest increases of atmospheric concentrations of toxic heavy metals (times with respect to TH) were: Cd (20–50), Cu (30–300), Pb (2–33), and Sb (5–80) and were found in those five distributed East−West along the NR5 and NR11 national roads, the Algiers−Blida railway, and the Houari Boumediene international airport. These elements and others (such as Ga, La, Cr, Cs, Ti, V, and Ce) were present in these zones at severe contamination levels (10–17 elements present at heavy contamination levels with CF $>$ 3) and found highly enriched at levels globally exceeding those reported in a number of comparable areas worldwide. Multivariate analysis scoring attempted to disentangle dominantly lithogenic (Al, Cr, Fe, Ti, Co, Rb, Sm, and Sc) vs. anthropogenic (e.g., Cd, Cu, Pb, Sb, V, and Zn) pollution sources, unsurprisingly tracing back to exploding human activity and vehicular density as key environmental causes. Expectedly, the finding that the wooded Reghaia Nature Reserve, located North-South with respect to the 'pollution axis', behaved as a green barrier further highlights the high overall ecological risk in the Rouiba−Reghaia region, and the usefulness of establishing periodic registers of multi-elemental airborne contamination.

## Credit author statement

**Henia Saib:** Conceptualization, Methodology, Investigation, Data curation, Writing – original draft. **Amine Yekkour:** Formal analysis. **Mohamed Toumi:** Resources. **Bouzid Guedioura:** Investigation, Data curation. **Mohamed Amine Benamar:** Resources. **Abdelhamid Zeghdaoui:** Investigation. **Annabelle Austruy:** Methodology, Resources. **David Bergé-Lefranc:** Formal analysis, Methodology. **Marcel Culcasi:** Formal analysis, Writing – review & editing, Visualization. **Sylvia Pietri:** Conceptualization, Project administration, Supervision, Funding acquisition, Writing – review & editing.

## Declaration of competing interest

The authors declare that they have no known competing financial interests or personal relationships that could have appeared to influence the work reported in this paper.

## Acknowledgements

Authors thank the Agence Nationale de la Recherche (ANR Mito-DiaPM – N° ANR-17-CE34-0006-01), the CNRS (Centre National de la Recherche Scientifique) and the French Higher Education and Research Ministry for funding part of this study. Authors wish to thank people at SIG office (for the conception and realization of the database) and at BNEDER (National Study Office for Rural Development) for contribution to the implementation of the map of study area. H.S. gratefully thanks people at NUR Research Reactor and Physics and Nuclear Application Division/CRND (Draria, Algeria) for experimental support, especially with irradiation procedures. Ms. L. Diaz (University of Pau, France) is gratefully acknowledged for her valuable contribution to this paper.

## Appendix ASupplementary data

Supplementary data to this article can be found online at https://doi.org/10.1016/j.apr.2022.101643.

## References

Adamo, P., Giordano, S., Vingiani, S., Castaldo Cobianchi, R., Violante, P., 2003. Trace element accumulation by moss and lichen exposed in bags in the city of Naples (Italy). Environ. Pollut. 122, 91–103. https://doi.org/10.1016/S0269-7491(02)00277-4.

Adjiri, F., Ramdani, M., Iograda, T., Chalard, P., 2018. Bio-monitoring of metal trace elements by epiphytic lichen in the Bordj BouArreridj area, east of Algeria. Der Pharma Chem. 10 (3), 1–8.

Agnan, Y., Séjalon-Delmas, N., Probst, A., 2013. Comparing early twentieth century and present-day atmospheric pollution in SW France: a story of lichens. Environ. Pollut. 172, 139–148. https://doi.org/10.1016/j.envpol.2012.09.008.

Agnan, Y., Séjalon-Delmas, N., Claustres, A., Probst, A., 2015. Investigation of spatial and temporal metal atmospheric deposition in France through lichen and moss bioaccumulation over one century. Sci. Total Environ. 529, 285–296. https://doi.org/10.1016/j.scitotenv.2015.05.083.

Agnan, Y., Séjalon-Delmas, N., Probst, A., 2017. Evaluation of lichen species resistance to atmospheric metal pollution by coupling diversity and bioaccumulation approaches: a new bioindication scale for French forested areas. Ecol. Indicat. 72, 99–110. https://doi.org/10.1016/j.ecolind.2016.08.006.

Ancora, S., Dei, R., Rota, E., Mariotti, G., Bianchi, N., Bargagli, R., 2021. Altitudinal variation of trace elements deposition in forest ecosystems along the NW side of Mt. Amiata (central Italy): evidence from topsoil, mosses and epiphytic lichens. Atmos. Pollut. Res. 12, 101200 https://doi.org/10.1016/j.apr.2021.101200.

Aslan, A., Gurbuz, H., Yazici, K., Cicek, A., Turan, M., Ercisli, S., 2013. Evaluation of lichens as bio-indicators of metal pollution. J. Elem. 18, 353–369. https://doi.org/10.5601/jelem.2013.18.3.01.

Austruy, A., Yung, L., Ambrosi, J.P., Girardclos, O., Keller, C., Angeletti, B., Dron, J., Chamaret, P., Chalot, M., 2019. Evaluation of historical atmospheric pollution in an industrial area by dendrochemical approaches. Chemosphere 220, 116–126. https://doi.org/10.1016/j.chemosphere.2018.12.072.

Bajpai, R., Upreti, D., 2012. Accumulation and toxic effect of arsenic and other heavy metals in a contaminated area of West Bengal, India, in the lichen *Pyxine cocoes* (Sw.). Nyl. Ecotox. Environ. Safe. 83, 63–70. https://doi.org/10.1016/j.ecoenv.2012.06.001.

Baraldi, R., Chieco, C., Neri, L., Facini, O., Rapparini, F., Morrone, L., Carriero, G., 2019. An integrated study on air mitigation potential of urban vegetation: from a multi-trait approach to modeling. Urban For. Urban Green. 41, 127–138. https://doi.org/10.1016/j.ufug.2019.03.020.

Bari, A., Rosso, A., Minciardi, M.R., Troiani, F., Piervittori, R., 2001. Analysis of heavy metals in atmospheric particulates in relation to their bioaccumulation in explanted *Pseudevernia furfuracea* thalli. Environ. Monit. Assess. 69, 205–220. https://doi.org/10.1023/A:1010757924363.

Basile, A., Sorbo, S., Aprile, G.G., Conte, B., Castaldo Cobianchi, R., 2008. Comparison of the heavy metal bioaccumulation capacity of an epiphytic moss and an epiphytic lichen. Environ. Pollut. 151, 401–407. https://doi.org/10.1016/j.envpol.2007.07.004.

Bergamaschi, L., Rizzio, E., Giaveri, G., Profumo, A., Loppi, S., Gallorini, M., 2004. Determination of baseline element composition of lichens using samples from high elevations. Chemosphere 55, 933–939. https://doi.org/10.1016/j.chemosphere.2003.12.010.

Boamponsem, L.K., Adam, J.I., Dampare, S.B., Nyarko, B.J.B., Essumang, D.K., 2010. Assessment of atmospheric heavy metal deposition in the Tarkwa gold mining area of Ghana using epiphytic lichens. Nucl. Instrum. Methods Phys. Res. B 268, 1492–1501. https://doi.org/10.1016/j.nimb.2010.01.007.

Boamponsem, L.K., De Freitas, C.R., Williams, D., 2017. Source apportionment of air pollutants in the Greater Auckland Region of New Zealand using receptor models and elemental levels in the lichen, *Parmotrema reticulatum*. Atmos. Pollut. Res. 8, 101–113. https://doi.org/10.1016/j.apr.2016.07.012.

Boonpeng, C., Polyiam, W., Sriviboon, C., Sangiamdee, D., Watthana, S., Nimis, P., Boonpragob, K., 2017. Airborne trace elements near a petrochemical industrial complex in Thailand assessed by the lichen *Parmotrema tinctorum* (Despr. ex Nyl.) Hale. Environ. Sci. Pollut. Res. 24, 12393–12404. https://doi.org/10.1007/s11356-017-8893-9.

Bouhila, Z., Mouzai, M., Azli, T., Nedjar, A., Mazouzi, C., Zergoug, Z., Boukhadra, D., Chegrouche, S., Lounici, H., 2015. Investigation of aerosol trace element concentrations nearby Algiers for environmental monitoring using instrumental neutron activation analysis. Atmos. Res. 166, 49–59. https://doi.org/10.1016/j.atmosres.2015.06.013.

Bozkurt, Z., 2017. Determination of airborne trace elements in an urban area using lichens as biomonitor. Environ. Monit. Assess. 189, 573. https://doi.org/10.1007/s10661-017-6275-x.

Bruinen de Bruin, Y., Koistinen, K., Yli-Tuomi, T., Kephalopoulos, S., Jantunen, M., 2006. A Review of Source Apportionment Techniques and Marker Substances Available for Identification of Personal Exposure, Indoor and Outdoor Sources of Chemicals. Joint Research Centre Institute for Health and Consumer Protection, Publication Office of the European Commission, Directorate General. EUR 22349EN.

Brunialti, G., Frati, L., 2007. Biomonitoring of nine elements by the lichen Xanthoria parietina in Adriatic Italy: a retrospective study over a 7-year time span. Sci. Total Environ. 387, 289–300. https://doi.org/10.1016/j.scitotenv.2007.06.033.

Contardo, T., Vannini, A., Sharma, K., Giordani, P., Loppi, S., 2020. Disentangling sources of trace element air pollution in complex urban areas by lichen biomonitoring. A case study in Milan (Italy). Chemosphere 256, 127155. https://doi.org/10.1016/j.chemosphere.2020.127155.

Conti, M.E., Cecchetti, G., 2001. Biological monitoring: lichens as bioindicators of air pollution assessment - a review. Environ. Pollut. 114, 471–492. https://doi.org/10.1016/S0269-7491(00)00224-4.

Culicov, O.A., Yurukova, L.D., 2006. Comparison of element accumulation of different moss- and lichen-bags, exposed in the city of Sofia (Bulgaria). J. Atmos. Chem. 55, 1–12. https://doi.org/10.1007/s10874-005-9002-x.

Cuny, D., Van Haluwyn, C., Pesch, R., 2001. Biomonitoring of trace elements in air and soil compartments along the motorway in France. Water Air Soil Pollut. 125, 273–289. https://doi.org/10.1023/A:1005278900969.

de Bruin, M., 1990. Applying biological monitors and neutron activation analysis in studies of heavy-metal air pollution. Moss, tree bark, lichens and other materials can yield important information about environmental pollution and its likely sources. IAEA Bull. 4, 22–27.

Demiray, A.D., Yolcubal, I., Akyol, N.H., Cobanoglu, G., 2012. Biomonitoring of airborne metals using the lichen Xanthoria parietina in Kocaeli Province, Turkey. Ecol. Indicat. 18, 632–643. https://doi.org/10.1016/j.ecolind.2012.01.024.

Demková, L., Baranová, B., Oboňa, J., Árvay, J., Lošák, T., 2017. Assessment of air pollution by toxic elements on petrol stations using moss and lichen bag technique. Plant Soil Environ. 8, 355–361. https://doi.org/10.17221/297/2017-PSE.

Dong, S., Gonzalez, R.O., Harrison, R.M., Green, D., North, R., Fowler, G., Weiss, D., 2017. Isotopic signatures suggest important contributions from recycled gasoline, road dust and non-exhaust traffic sources for copper, zinc and lead in PM10 in London, United Kingdom. Atmos. Environ. 165, 88–98. https://doi.org/10.1016/j.atmosenv.2017.06.020.

Dron, J., Ratier, A., Austruy, A., Revenko, G., Chaspoul, F., Wafo, E., 2021. Effect of meteorological conditions and topography on the bioaccumulation of PAHs and metal elements by native lichen (Xanthoria parietina). J. Environ. Sci. 109, 193–205. https://doi.org/10.1016/j.jes.2021.03.045.

Enamorado-Báez, S.M., Gómez-Guzmán, J.M., Chamizo, E., Abril, J.M., 2015. Levels of 25 trace elements in high-volume air filter samples from Seville (2001–2002): sources, enrichment factors and temporal variations. Atmos. Res. 155, 118–129. https://doi.org/10.1016/j.atmosres.2014.12.005.

Filzmoser, P., Reimann, C., 2002. Robust multivariate methods in geostatistics. In: Gaul, W., Ritter, G. (Eds.), Classification, Automation, and New Media. Studies in Classification, Data Analysis, and Knowledge Organization. Springer, Berlin, Heidelberg. https://doi.org/10.1007/978-3-642-55991-4_46.

Frati, L., Brunialti, G., Loppi, S., 2005. Problems related to lichen transplants to monitor trace element deposition in repeated surveys: a case study from central Italy. J. Atmos. Chem. 52, 221–230. https://doi.org/10.1007/s10874-005-3483-5.

Freitas, M.C., Catarino, F.M., Branquinho, C., Maguas, C., 1993. Preparation of a lichen reference material. J. Radioanal. Nucl. Chem. 169, 47–55. https://doi.org/10.1007/BF02046782.

Fujiwara, F., Rebagliati, R.J., Marrero, J., Gomez, D., Smichowski, P., 2011. Antimony as a traffic-related element in size-fractionated road dust samples collected in Buenos Aires. Microchem. J. 97, 62–67. https://doi.org/10.1016/j.microc.2010.05.006.

Gallo, L., Corapi, A., Loppi, S., Lucadamo, L., 2014. Element concentrations in the lichen *Pseudevernia furfuracea* (L.) Zopf transplanted around a cement factory (S Italy). Ecol. Indicat. 46, 566–574. https://doi.org/10.1016/j.ecolind.2014.07.029.

Garty, J., Weissman, L., Tamir, O., Beer, S., Cohen, Y., Karnieli, A., Orlovsky, L., 2000. Comparison of five physiological parameters to assess the vitality of the lichen Ramalina lacera exposed to air pollution. Physiol. Plantarum 109 (4), 410–418. https://doi:10.1034/j.1399-3054.2000.100407.x.

Giampaoli, P., Wannaz, E.D., Tavares, A.R., Domingos, M., 2016. Suitability of Tillandsia usneoides and Aechmea fasciata for biomonitoring toxic elements under tropical seasonal climate. Chemosphere 149, 14–23. https://doi.org/10.1016/j.chemosphere.2016.01.080.

Gianini, M., Fischer, A., Gehrig, R., Ulrich, A., Wichser, A., Piot, C., Hueglin, C., 2012. Comparative source apportionment of PM10 in Switzerland for 2008/2009 and 1998/1999 by positive matrix factorisation. Atmos. Environ. 54, 149–158. https://doi.org/10.1016/j.atmosenv.2012.02.036.

Greenacre, M., 2017. Correspondence analysis in practice. In: Interdisciplinary Statistics Series, third ed. Chapman & Hall/CRC, New York. https://doi.org/10.1201/9781315369983.

Guedioura, B., Bendjaballah, N., Alioui, N., 2014. Profiling measurements of metal ion distribution in thin polymer inclusion membranes by Rutherford backscattering spectrometry. Radiat. Eff. Defect Solid 169, 388–395. https://doi.org/10.1080/10420150.2013.865621.

Guidotti, M., Stella, D., Dominici, C., Blasi, G., Owczarek, M., Vitali, M., Protano, C., 2009. Monitoring of traffic-related pollution in a province of central Italy with transplanted lichen *Pseudovernia furfuracea*. Bull. Environ. Contam. Toxicol. 83, 852–858. https://doi.org/10.1007/s00128-009-9792-7.

Herrero Fernández, Z., Estevez Álvarez, J.R., Montero Álvarez, A., Pupo González, I., dos Santos Júnior, J.A., Ortueta Milan, M., Padilla Álvarez, R., 2015. Multielement analysis of lichen samples using XRF methods. Comparison with ICP-AES and FAAS. X Ray Spectrom. 45, 77–84. https://doi.org/10.1002/xrs.2657.

Humerovic, J., Muhic-Sarac, T., Memic, M., Zero, S., Selovic, A., 2015. Multielement and rare earth element composition of the soil and lichen from Sarajevo, Bosnia and Herzegovina. Ekoloji 24, 36–44. https://doi.org/10.5053/ekoloji.2015.10.

Incerti, G., Cecconi, E., Capozzi, F., Adamo, P., Bargagli, R., Benesperi, R., Carniel, F.C., Cristofolini, F.S., Giordano, S., Puntillo, D., Spagnuolo, V., Tretiach, M., 2017. Infraspecific variability in baseline element composition of the epiphytic lichen *Pseudevernia furfuracea* in remote areas: implications for biomonitoring of air pollution. Environ. Sci. Pollut. Res. 24, 8004–8016. https://doi.org/10.1007/s11356-017-8486-7.

Kim, H., Harrison, F.E., Aschner, M., Bowman, A.B., 2022. Exposing the role of metals in neurological disoders: a focus on manganese. Trends Mol. Med. 28, 555–568. https://doi.org/10.1016/j.molmed.2022.04.011.

Kłos, A., Rajfur, M., Wacławek, M., 2011. Application of enrichment factor (EF) to the interpretation of results from the biomonitoring studies. Ecol. Chem. Eng. S18, 171–183. https://doi.org/10.1016/j.molmed.2022.04.011.

Kodnik, D., Winkler, A., Carniel, F.C., Tretiach, M., 2017. Biomagnetic monitoring and element content of lichen transplants in a mixed land use area of NE Italy. Sci. Total Environ. 595, 858–867. https://doi.org/10.1016/j.scitotenv.2017.03.261.

Lê, S., Josse, J., Husson, F., 2008. FactoMineR: an R package for multivariate analysis. J. Stat. Software 25, 1–18. https://doi.org/10.18637/jss.v025.i01.

Legendre, P., Legendre, L., 1998. Numerical Ecology, second ed. Elsevier Science Ltd., Amsterdam.

Levin, R., Zilli Vieira, C.L., Rosenbaum, M.H., Bischoff, K., Mordarski, D.C., Brown, M.J., 2021. The urban lead (Pb) burden in humans, animals and the natural environment. Environ. Res. 193, 110377 https://doi.org/10.1016/j.envres.2020.110377.

CRC handbook of chemistry and Physics, section 14: geophysics, astronomy and acoustics. In: Lide, D.R. (Ed.), 2005. Abundance of Elements in the Earth's Crust and in the Sea, 85th Ed. CRC Press, Boca Raton, FL, USA.

López Berdonces, M.A., Higueras, P.L., Fernández-Pascual, M., Borreguero, A.M., Carmona, M., 2017. The role of native lichens in the biomonitoring of gaseous mercury at contaminated sites. J. Environ. Manag. 15 (186), 207–213. https://doi.org/10.1016/j.jenvman.2016.04.047.

Loppi, S., Corsini, A., 2003. Diversity of epiphytic lichens and metal contents of *Parmelia caperata* thalli as monitors of air pollution in the town of Pistoia. Environ. Monit. Assess. 86, 289–301. https://doi.org/10.1023/A:1024017118462.

Loppi, S., Frati, L., Paoli, L., Bigagli, V., Rossetti, C., Bruscoli, C., Corsini, A., 2004. Biodiversity of epiphytic lichens and heavy metal contents of *Flavoparmelia caperata* thalli as indicators of temporal variations of air pollution in the town of Montecatini Terme (central Italy). Sci. Total Environ. 326, 113–122. https://doi:10.1016/j.scitotenv.2003.12.003.

Lough, G.C., Schauer, J.J., Park, J.S., Shafer, M.M., DeMinter, J.T., Weinstein, J.P., 2005. Emissions of metals associated with motor vehicle roadways. Environ. Sci. Technol. 39, 826–836. https://doi.org/10.1021/es048715f.

Lucadamo, L., Corapi, A., Loppi, S., De Rosa, R., Barca, D., Vespasiano, G., Gallo, L., 2016. Spatial variation in the accumulation of elements in thalli of the lichen *Pseudevernia furfuracea* (L.) Zopf transplanted around a biomass power plant in Italy. Arch. Environ. Contam. Toxicol. 70, 506–521. https://doi.org/10.1007/s00244-015-0238-4.

Lucadamo, L., Gallo, L., Corapi, A., 2022. Detection of air quality improvement within a suburban district (southern Italy) by means of lichen biomonitoring. Atmos. Pollut. Res. 13, 101346 https://doi.org/10.1016/j.apr.2022.101346.

Maatoug, M., Medkour, K., Ait Hammou, M., Ayad, N., 2010. Cartography of atmospheric pollution by the lead from road traffic using transplantation of a lichen bioaccumulator Xanthoria Parietina in Tiaret city (Algeria). Pollut. Atmos. 205, 93–101. https://doi.org/10.4267/pollution-atmospherique.734.

Malaspina, P., Giordania, P., Modenesi, P., Abelmoschi, M.L., Magi, E., Soggia, F., 2014. Bioaccumulation capacity of two chemical varieties of the lichen Pseudevernia furfuracea. Ecol. Indicat. 45, 605–610. https://doi.org/10.1016/j.ecolind.2014.05.026.

Massimi, L., Conti, M.E., Mele, G., Ristorini, M., Astolfi, M.L., Canepari, S., 2019. Lichen transplants as indicators of atmospheric element concentrations: a high spatial resolution comparison with PM10 samples in a polluted area (Central Italy). Ecol. Indicat. 101, 759–769. https://doi.org/10.1016/j.ecolind.2018.12.051.

Nannoni, F., Santolini, R., Protano, G., 2015. Heavy element accumulation in *Evernia prunastri* lichen transplants around a municipal solid waste landfill in central Italy. Waste Manage. (Tucson, Ariz.) 43, 353–362. https://doi.org/10.1016/j.wasman.2015.06.013.

Olowoyo, J., van Heerden, E., Fischer, J.L., 2011. Trace element concentrations from lichen transplants in Pretoria, South Africa. Environ. Sci. Pollut. Res. 18, 663–668. https://doi.org/10.1007/s11356-010-0410-3.

Osyczka, P., Boroń, P., Lenart-Boroń, A., Rola, K., 2018. Modifications in the structure of the lichen Cladonia thallus in the aftermath of habitat contamination and implications for its heavy-metal accumulation capacity. Environ. Sci. Pollut. Res. 25, 1950–1961. https://doi.org/10.1007/s11356-017-0639-1.

Pacheco, A.M.G., Freitas, M.C., 2009. Trace-element enrichment in epiphytic lichens and tree bark at Pico Island, Azores, Portugal. J. Air Waste Manage. Assoc. 59, 411–418. https://doi.org/10.3155/1047-3289.59.4.411.

Pacyna, J.M., Pacyna, E.G., 2001. An assessment of global and regional emissions of trace metals to the atmosphere from anthropogenic sources worldwide. Environ. Rev. 9, 269–298. https://doi.org/10.1139/a01-012.

Pantelica, A., Cercasov, V., Steinnes, E., Bode, P., Wolterbeek, H., 2016. Determination of 54 elements in lichen transplants: comparison of INAA, ICPMS, and EDXRF. Rom. J. Phys. 61, 1380–1388.

Paoli, L., Munzi, S., Fiorini, E., Gaggi, C., Loppi, S., 2013. Influence of angular exposure and proximity to vehicular traffic on the diversity of epiphytic lichens and the bioaccumulation of traffic-related elements. Environ. Sci. Pollut. Res. 20, 250–259. https://doi.org/10.1007/s11356-012-0893-1.

Paoli, L., Munzi, S., Guttová, A., Senko, D., Sardella, G., Loppi, S., 2015. Lichens as suitable indicators of the biological effects of atmospheric pollutants around a municipal solid waste incinerator (S Italy). Ecol. Indicat. 52, 362–370. https://doi.org/10.1016/j.ecolind.2014.12.018.

Parviainen, A., Papaslioti, E.M., Casares-Porcel, M., Garrido, C.J., 2020. Antimony as a tracer of non-exhaust traffic emissions in air pollution in Granada (S Spain) using lichen bioindicators. Environ. Pollut. 263, 114482. https://doi:10.1016/j.envpol.2020.114482.

Perez Catán, S., Bubach, D., Messuti, M.I., Arribére, M.A., Guevara, S.R., 2020. Mercury in a geothermal and volcanic area in Patagonia, southern South America. Atmos. Pollut. Res. 11, 566–573. https://doi.org/10.1016/j.apr.2019.12.005.

Rahali, M., 2002. Mapping of lead pollution in Algiers area with a lichen *(Xanthoria parietina)* as indicator. Pollut. Atmos. 175, 421–432. https://doi.org/10.4267/pollution-atmospherique.2605.

Ratier, A., Dron, J., Revenko, G., Austruy, A., Dauphin, C.E., Chaspoul, F., Wafo, E., 2018. Characterization of atmospheric emission sources in lichen from metal and organic contaminant patterns. Environ. Sci. Pollut. Res. 25, 8364–8376. https://doi.org/10.1007/s11356-017-1173-x.

Rehman, K., Fatima, F., Waheed, I., Hamid Akach, M.S., 2018. Prevalence of exposure of heavy metals and their impact on health consequences. J. Cell. Biochem. 119, 157–184. https://doi.org/10.1002/jcb.26234.

Reiman, C., de Caritat, P., 2000. Intrinsic flaws of element enrichment factors (Efs) in environmental geochemistry. Environ. Sci. Technol. 34, 5084–5091. https://doi.org/10.1021/es001339o.

Rekik, B., Derbal, M., Lebbou, K., Benammar, M.E.A., 2016. Yb3þ-doped LiBi $(WO_4)_2$ single crystals fibers grown by micro-pulling down technique and characterization. J. Cryst. Growth 452, 101–104, 10.1016%2Fj.jcrysgro.2016.03.022.

Rola, K., Osyczka, P., 2019. Temporal changes in accumulation of trace metals in vegetative and generative parts of Xanthoria parietina lichen thalli and their implications for biomonitoring studies. Ecol. Indicat. 96, 293–302. https://doi.org/10.1016/j.ecolind.2018.09.004.

Saiki, M., Chaparro, C.G., Vasconcellos, M.B.A., Marcelli, M.P., 1997. Determination of trace elements in lichens by instrumental neutron activation analysis. J. Radioanal. Nucl. Chem. 217, 111–115. https://doi.org/10.1007/BF02055358.

Scerbo, R., Ristori, T., Possentin, L., Lampugnani, L., Barale, R., Barghigiani, C., 2002. Lichen (*Xanthoria parietina*) biomonitoring of trace element contamination and air quality assessment in Pisa Province (Tuscany, Italy). Sci. Total Environ. 286, 27–40. https://doi.org/10.1016/s0048-9697(01)00959-7.

Semadi, A., 1994. Lead pollution monitoring by transplanted lichens in Annaba area (Algeria). Pollut. Atmos. 140, 86–102.

Sorbo, S., Aprile, G., Strumia, S., Castaldo Cobianchi, R., Leoned, A., Basile, A., 2008. Trace element accumulation in *Pseudevernia furfuracea* (L.) Zopf exposed in Italy's so-called Triangle of Death. Sci. Total Environ. 407, 647–654. https://doi.org/10.1016/j.scitotenv.2008.07.071.

Swanton, C., Hill, W., Lim, E., Lee, C., Weeden, C.E., Augustine, M., Chen, K., Kuan, F.C., Marongiu, F., Rodrigues, F., Cha, H., Jacks, T., Luchtenborg, M., Malanchi, I., Downward, J., Carlsten, C., Hackshaw, A., Litchfield, K.R., DeGregori, J., Jamal-Hanjani, M., 2022. Mechanism of action and an actionable inflammatory axis for air pollution induced non-small cell lung cancer: towards molecular cancer prevention. Ann. Oncol. 33, S1413. https://doi.org/10.1016/j.annonc.2022.08.046. Sup. 7.

Vannini, A., Paoli, L., Russo, A., Loppi, S., 2019. Contribution of submicronic (PM1) and coarse (PM> 1) particulate matter deposition to the heavy metal load of lichens transplanted along a busy road. Chemosphere 231, 121–125. https://doi.org/10.1016/j.chemosphere.2019.05.085.

Vuković, G., Urošević, M.A., Škrivanj, S., Milićević, T., Dimitrijević, D., Tomašević, M., Popović, A., 2016. Moss bag biomonitoring of airborne toxic element decrease on a small scale: a street study in Belgrade, Serbia. Sci. Total Environ. 542, 394–403. https://doi.org/10.1016/j.scitotenv.2015.10.091.

White, S.J.O., Shine, J.P., 2016. Exposure potential and health impacts of indium and gallium, metals critical to emerging electronics and energy technologies. Curr. Environ. Health Rep. 3, 459–467. https://doi.org/10.1007/s40572-016-0118-8.

Wu, Y.Y., Gao, J., Zhang, G.Z., Zhao, R.K., Liu, A.Q., Sun, L.W., Li, X., Tang, H.L., Zhao, L.C., Guo, X.P., Liu, H.J., 2020. Two lichens differing in element concentrations have similar spatial patterns of element concentrations responding to road traffic and soil input. Sci. Rep. 10, 19001 https://doi.org/10.1038/s41598-020-76099-x.

Xiong, Q., Zhao, W., Zhao, J., Zhao, W., Jiang, L., 2017. Concentration levels, pollution characteristics and potential ecological risk of dust heavy metals in the metropolitan area of Beijing, China. Int. J. Environ. Res. Publ. Health 14, 1159. https://doi.org/10.3390/ijerph14101159.

Zechmeister, H.G., Hohenwallner, D., Riss, A., Hanus-Illnar, A., 2005. Estimation of element deposition derived from road traffic sources by using mosses. Environ. Pollut. 138, 238–249. https://doi.org/10.1016/j.envpol.2005.04.005.

Zeng, X., Liu, Y., You, S., Zeng, G., Tan, X., Hu, X., Huang, L., Li, F., 2015. Spatial distribution, health risk assessment and statistical source identification of the trace elements in surface water from the Xiangjiang river, China. Environ. Sci. Pollut. Res. 22, 9400–9412. https://doi.org/10.1007/s11356-014-4064-4.

Zhao, L., Zhang, C., Jia, S., Liu, Q., Chen, Q., Li, X., Liu, X., Wu, Q., Zhao, L., Liu, H., 2019. Element bioaccumulation in lichens transplanted along two roads: the source and integration time of elements. Ecol. Indicat. 99, 101–110. https://doi.org/10.1016/j.ecolind.2018.12.020.

Zhou, Y., Niu, L., Liu, K., Yin, S., Liu, W., 2018. Arsenic in agricultural soils across China: distributiion pattern, accumulation trend, influencing factors, and risk assessment. Sci. Total Environ. 156–163. https://doi.org/10.1016/j.scitotenv.2017.10.232, 616–617.